Med

Article

Clinically actionable genomic and transcriptomic landscape of advanced neuroendocrine neoplasms

Graphical abstract

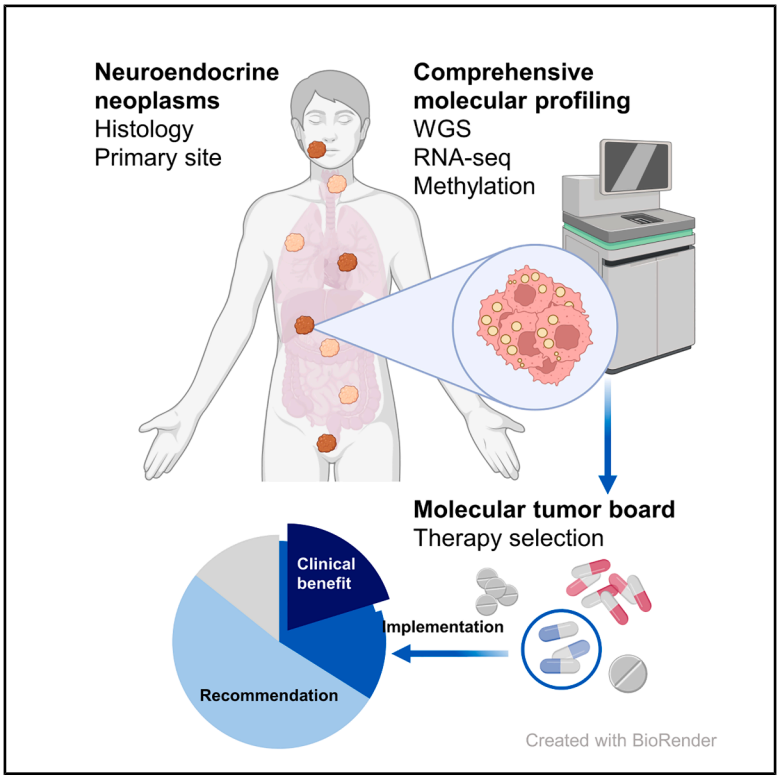

Authors

Simon Kreutzfeldt, Leonidas Apostolidis, Małgorzata Oleś, ..., Peter Horak, Hanno Glimm, Stefan Fröhling

Correspondence

stefan.froehling@nct-heidelberg.de

In brief

Neuroendocrine neoplasms (NENs) represent a diverse group of cancers with substantial unmet clinical need. Kreutzfeldt, Apostolidis, Oleś, et al. show that comprehensive genomic and transcriptomic profiling in patients with advanced NENs yields actionable insights enabling effective personalized therapies, deepens our understanding of NEN biology, and facilitates innovative clinical management strategies.

Highlights

- Molecular profiling revealed alteration patterns in neuroendocrine neoplasms (NENs)
- Alteration patterns differed by tissue of origin and histologic subtype
- Profiling also identified actionable biomarkers, enabling individualized therapies
- Molecularly guided treatment yielded clinical benefit in 59.6% of treated patients

Translation to Patients

Kreutzfeldt et al., 2026, Med 7, 101130
June 12, 2026
https://doi.org/10.1016/j.medj.2026.101130

CellPress

Med

CellPress
OPEN ACCESS

Article

Clinically actionable genomic and transcriptomic landscape of advanced neuroendocrine neoplasms

Simon Kreutzfeldt,[1,2,3,34] Leonidas Apostolidis,[2,4,34] Małgorzata Oleś,[5,34] Eva Krieghoff-Henning,[1,2,6,7,8] Christoph E. Heilig,[1,2,3] Christoph Heining,[9,10,11] Andreas Mock,[1,2,12,13] Maria-Veronica Teleanu,[1,2,3] Barbara Hutter,[5] Laura Gieldon,[14,15,16] Barbara Klink,[14,17,18] Katja Beck,[1,2] Daniela Richter,[9,10] Annika Baude-Müller,[1,2] Eva Reisinger,[1,2] Nils Hammer,[1,2] Leila Kamkar,[1,2] Katrin Pfütze,[2] Christina Geörg,[2] Mario Lamping,[19,20,21] Damian T. Rieke,[19,20,21] Sebastian Uhrig,[5] Henning Jann,[22,23] Ulrich-Frank Pape,[22,24] Michael Allgäuer,[25] Albrecht Stenzinger,[25] Eva C. Winkler,[2,4] Bertram Wiedenmann,[22] Dirk Jäger,[2,4] Benedikt Brors,[3,26] Daniel Hübschmann,[2,3,5,27,28] Evelin Schröck,[11,14,15,29] Ulrich Keilholz,[20,21] Marianne Pavel,[22,30,33] Peter Horak,[1,2,3,33] Hanno Glimm,[9,10,11,31,33] and Stefan Fröhling[1,2,3,32,33,35,*]

[1]Division of Translational Medical Oncology, German Cancer Research Center (DKFZ), Heidelberg, Germany
[2]National Center for Tumor Diseases (NCT), NCT Heidelberg, a partnership between DKFZ and Heidelberg University Hospital, Heidelberg, Germany
[3]German Cancer Consortium (DKTK), Core Center Heidelberg, Heidelberg, Germany
[4]Department of Medical Oncology, Heidelberg University Hospital, Heidelberg, Germany
[5]Computational Oncology Group, Molecular Precision Oncology Program, NCT Heidelberg and DKFZ, Heidelberg, Germany
[6]Division of Personalized Medical Oncology, DKFZ, Heidelberg, Germany
[7]Department of Personalized Oncology, DKFZ-Hector Cancer Institute, University Medical Center Mannheim, Medical Faculty Mannheim, Heidelberg University, Mannheim, Germany
[8]Department of Personalized Oncology, University Medical Center Mannheim, Medical Faculty Mannheim, Heidelberg University, Mannheim, Germany
[9]Department of Translational Medical Oncology, NCT, NCT/University Cancer Center Dresden, a partnership between DKFZ, Faculty of Medicine and University Hospital Carl Gustav Carus, Dresden University of Technology (TUD), and Helmholtz-Zentrum Dresden-Rossendorf, Dresden, Germany
[10]Translational Medical Oncology, Faculty of Medicine and University Hospital Carl Gustav Carus, TUD, Dresden, Germany
[11]DKTK, Partner Site Dresden, Dresden, Germany
[12]Institute of Pathology, Ludwig Maximilians University Munich, Munich, Germany
[13]DKTK, Partner Site Munich, Munich, Germany
[14]Institute for Clinical Genetics, Faculty of Medicine and University Hospital Carl Gustav Carus, TUD, and Hereditary Cancer Syndrome Center Dresden, Dresden, Germany
[15]European Reference Network for Genetic Tumour Risk Syndromes (ERN GENTURIS), Hereditary Cancer Syndrome Center Dresden, Dresden, Germany
[16]Institute of Medical Genetics, Carl von Ossietzky University, Oldenburg, Germany
[17]Medizinisch Genetisches Zentrum, Munich, Germany
[18]ERN GENTURIS, Nijmegen, the Netherlands
[19]Department of Hematology, Oncology and Cancer Immunology, Charité – Universitätsmedizin Berlin, Berlin, Germany
[20]Charité Comprehensive Cancer Center, Charité – Universitätsmedizin Berlin, Berlin, Germany
[21]DKTK, Partner Site Berlin, Berlin, Germany
[22]Department of Hepatology and Gastroenterology, Charité – Universitätsmedizin Berlin, Berlin, Germany
[23]Department of Internal Medicine – Gastroenterology, Hematology and Oncology, Nephrology, DRK Kliniken Berlin Köpenick, Berlin, Germany
[24]Berlin Institute of Health, Berlin, Germany
[25]Institute of Pathology, Heidelberg University Hospital, Heidelberg, Germany
[26]Division of Applied Bioinformatics, DKFZ, Heidelberg, Germany
[27]Innovation and Service Unit for Bioinformatics and Precision Medicine, DKFZ, Heidelberg, Germany
[28]Pattern Recognition and Digital Medicine Group, Heidelberg Institute for Stem Cell Technology and Experimental Medicine, Heidelberg, Germany
[29]Max Planck Institute of Molecular Cell Biology and Genetics, Dresden, Germany
[30]Department of Medicine 1, Division of Endocrinology, Friedrich Alexander University Erlangen-Nuremberg, Erlangen, Germany
[31]Translational Functional Cancer Genomics, DKFZ, Heidelberg, Germany
[32]Institute of Human Genetics, Heidelberg University, Heidelberg, Germany
[33]Senior author
[34]These authors contributed equally
[35]Lead contact
*Correspondence: stefan.froehling@nct-heidelberg.de
https://doi.org/10.1016/j.medj.2026.101130

CONTEXT AND SIGNIFICANCE Neuroendocrine neoplasms (NENs) are a diverse group of cancers that are still difficult to treat, especially at advanced stages. Detailed molecular analyses of these tumors have not been routinely integrated into clinical care. Our study shows that analyses of genetic changes and gene activity in patients with advanced NENs lead to the detection of additional therapeutic targets, both directly for the individual patient and—more indirectly—for future patients by improving our knowledge on typical NEN characteristics and vulnerabilities.

SUMMARY

Background: Epithelial neuroendocrine neoplasms (NENs) are a rare and heterogeneous group of malignancies with limited treatment options. Comprehensive molecular characterization may reveal novel therapeutic opportunities for these clinically challenging tumors.
Methods: Within a nationwide precision oncology program, we performed whole-genome/exome and transcriptome sequencing in 168 patients with a diagnosis of advanced NEN from diverse anatomic origins, followed by evaluation of real-world outcomes associated with molecularly guided interventions.
Findings: Our analysis revealed substantial molecular heterogeneity across advanced NENs, including distinct genetic profiles between low-grade and high-grade tumors, as well as alterations specific to particular tissues of origin. Candidate therapeutic targets included elevated tumor mutational burden induced by temozolomide exposure, rare actionable kinase mutations, overexpression of targetable antigens, and signatures of homologous recombination deficiency, providing a rationale for immune checkpoint blockade, kinase inhibitors, antibody-drug conjugates, poly(ADP-ribose) polymerase (PARP) inhibitors, and platinum-based therapies, respectively. Overall, 144 patients (85.7%) received molecularly guided treatment recommendations, of which 85 were implemented in 57 patients (39.6%). Among 68 evaluable therapy outcomes, 47 (69.1%) demonstrated clinical benefit (objective response, $n = 25$; disease stabilization, $n = 22$). At the patient level, 34 of the 57 treated (59.6%) experienced clinical benefit from at least one therapy (objective response, $n = 18$; disease stabilization, $n = 16$).
Conclusions: Comprehensive genomic and transcriptomic profiling identified distinct molecular alteration patterns and therapeutic vulnerabilities among different classes of epithelial NENs from various tissues, warranting further investigation in anatomic-site-specific studies. Our outcome data underscore the clinical utility of broad molecular profiling in patients with advanced NENs lacking further standard treatment options.
Funding: Funding for the study was institutional.

INTRODUCTION

Patients with rare cancers, including neuroendocrine neoplasms (NENs), face significant clinical challenges due to limited treatment options.[1,2] Comprehensive molecular profiling can identify key genetic drivers of such malignancies, potentially guiding targeted therapies.[3] This approach represents a shift from conventional management based solely on histopathologic and clinical features toward personalized interventions tailored to a tumor's unique molecular landscape.[4] When implemented through structured precision oncology programs, multi-layered tumor profiling proves especially valuable for rare cancers, as it not only expands therapeutic options for individual patients but also aggregates data from larger cohorts, enabling systematic insights that drive preclinical research and spur the development of novel treatments.[5]

Clinical trials in patients with NENs have traditionally relied on evolving histopathologic categories—low-grade (G1 or G2) neuroendocrine tumors (NETs), including lung carcinoid tumor; high-grade (G3) NETs; neuroendocrine carcinoma (NEC); and mixed neuroendocrine non-NENs (MiNENs)—as well as common sites of tumor origin, such as the pancreas, lung, and gastrointestinal tract, although NENs can arise in almost any location.[5,6] Consequently, established systemic therapies (somatostatin analogs, peptide receptor radionuclide therapy [PRRT], the mTOR inhibitor everolimus, the multi-tyrosine kinase inhibitor sunitinib, and chemotherapy) have primarily been evaluated based on broad morphologic criteria and the most frequent tumor sites, leaving the benefit for patients with rarer subtypes unclear.

In contrast, the potential of comprehensive molecular diagnostics to guide existing therapies or inform novel approaches tailored to individual tumor profiles remains largely unexplored, although genetic analyses have substantially refined our understanding of NEN biology.[1] Some hereditary and somatic alterations underlying NEN pathogenesis, most notably in *MEN1*, have been recognized for decades.[7,8] Recent advances in molecular profiling have revealed subtype-specific mutations

affecting *DAXX* and *ATRX* (pancreatic NETs), *CDKN1B* (small intestinal NETs), and the SWI/SNF complex (lung carcinoid tumor).[9–13] Additional site-specific mutations, such as those in *KRAS*, *APC*, and *BRAF* (common in the pancreas and colon) or *EGFR*, *STK11*, and *KEAP1* (predominant in the lung), likely reflect the transformation of ''classical'' carcinomas, further complicating the molecular landscape of NENs.[3] Moreover, grading-based analyses have highlighted key differences between G3 NETs and NECs, with the latter often displaying complex genomic profiles characterized by *TP53* and *RB1* loss, hallmarks associated with more aggressive behavior and poorer prognosis.[14–16] Proposed genomic and transcriptomic categories for select entities, such as small cell lung cancer,[17] and evidence of prognostic molecular subsets in pancreatic and small intestinal NETs[18,19] underscore the potential of genetically informed classification approaches. Finally, distinct transcriptional subtypes of NECs spanning various lineages and morphologies have recently been described.[20]

Translating molecular insights into more refined NEN therapies remains challenging for two main reasons. First, many NEN-driving mutations are not yet targetable, creating a gap between discovery and therapeutic application. Second, the rarity and heterogeneity of NENs complicate the design of sufficiently powered clinical trials, especially for subtype-specific interventions. While basket trials and other innovative study designs have advanced molecularly targeted therapies across various cancer types, recruiting patients with rare tumors remains difficult. As an alternative to traditional, often protracted clinical trials, precision oncology programs leverage high-resolution tumor profiling to correlate individual biomarker profiles with therapeutic responses, thereby facilitating both molecularly guided clinical decision-making and the generation of new hypotheses for future clinical research. Previous efforts to apply such strategies in patients with NENs have included case studies and early-phase investigations employing subgenomic molecular profiling.[21–26]

In this study, we analyzed the comprehensive molecular profiles, clinical characteristics, and treatment outcomes of a diverse cohort of heavily pretreated patients with NENs enrolled in the MASTER (Molecularly Aided Stratification for Tumor Eradication Research; ClinicalTrials.gov: NCT05852522) program, conducted by the German Cancer Research Center (DKFZ), the National Center for Tumor Diseases (NCT), and the German Cancer Consortium (DKTK).[5,27] Our results demonstrate the utility of whole-genome or whole-exome sequencing (WGS/WES) and RNA sequencing (RNA-seq) in guiding personalized clinical management. Furthermore, we uncovered unexpected therapeutic vulnerabilities targetable with current or emerging agents, illustrating how precision oncology registries serve as powerful ''signal-finding'' platforms to inform molecularly stratified clinical trial design and catalyze the development of new treatment strategies.

RESULTS

Patient cohort

A total of 168 patients with advanced, treatment-refractory epithelial NENs were enrolled between 2014 and 2019 in the DKFZ/NCT/DKTK MASTER program, which employs comprehensive molecular profiling through WGS/WES and RNA-seq to inform clinical management.[5,27] A multi-institutional molecular tumor board (MTB) reviewed the data of 160 patients (95.2%), resulting in treatment recommendations for 144 (90%). Of these, 57 patients (39.6%) received at least one recommended therapy, with response data available for 50 (34.7%; Figure 1A). Sequential molecular analyses were performed in 17 patients to capture tumor evolution over time.

Gastroenteropancreatic tumors were the largest subgroup (n = 87), followed by NENs originating in the lung (n = 20), genitourinary tract (n = 20), thyroid (medullary thyroid carcinoma, n = 10), head and neck (n = 9), and gynecologic organs (n = 11, including neuroendocrine breast cancer). An additional nine patients had NENs of unknown primary site (Figure 1B). Two cases (pat-166 and pat-168) were reclassified as non-NEN tumors following molecular profiling and were excluded from further analyses. Among the remaining 166 NENs, 75 (45.2%) were NECs, 21 (12.6%) were MiNENs, 22 (13.2%) were G3 NETs, and 48 (28.9%) were G1/2 NETs, demonstrating the cohort's heterogeneity. Primary tumor sites and grading for all patients are provided in Table S1. The median enrollment age was 49 years (range, 19–80), with an overall male predominance (61.9%), although the younger subgroup comprised a higher proportion of women (Figure 1C). Patients had received a median of three palliative therapies (range, 1–11) before molecular analysis, encompassing all modalities, including approved systemic treatments, immune checkpoint blockade, and poly(ADP-ribose) polymerase (PARP) inhibition (Figure 1C; Table S2). Objective response rates varied by tumor grade and drug class, rarely exceeding 30%; partial responses (PRs) were observed in G1/2 NETs after PRRT and in NECs or G3 NETs following chemotherapy (Figure 1B).

Genomic and transcriptomic landscape

We performed a cohort-wide analysis followed by stratification of tumors by histopathologic subtype, grade, and primary site to identify recurrent molecular alterations. Notably, certain categories defined by histopathologic subtype or grade were predominantly associated with specific primary tumor sites (Figure 1B): G3 NETs were almost exclusively of pancreaticobiliary origin, whereas the G1/2 NET cohort comprised approximately one-third gastrointestinal and one-third pancreaticobiliary tumors. Although the NEC and MiNEN cohorts were more heterogeneous, they still included relatively large proportions of gastrointestinal tumors. High-quality data were obtained for 160 patients (95.2%; WGS, n = 84; WES, n = 76; RNA-seq, n = 105). Overall, NENs showed a low median tumor mutational burden (TMB; 1.5 mutations per megabase [mut/Mb]; range, 0–480.9). Nevertheless, 21 cases (13.1%) exceeded 5 mut/Mb (defined as TMB high). Some of these had co-occurring somatic or germline alterations in *MSH6*, and in three cases, TMB reached several hundred mut/Mb. NECs and MiNENs had significantly higher TMB values than NETs, although all groups contained outliers (Wilcoxon rank-sum test; NEC vs. G1/2 NET $p = 2.2 \times 10^{-8}$; NEC vs. G3 NET, $p = 0.001$; Figure S1A).

Analyzing single-nucleotide variants (SNVs), insertions/deletions (indels), homozygous deletions, and amplifications revealed *TP53* as the most frequently altered gene (50 of 160

Figure 1. Patient cohort

(A) CONSORT diagram for enrollment, molecular diagnostics, clinical decision-making, and follow-up.

(B) Patient numbers according to tumor grade and primary tumor site (top), number of pre-MTB palliative therapies (middle), and best response to pre-MTB systemic therapies (bottom). CUP, carcinoma of unknown primary; SSTR, somatostatin receptor; CR, complete response; PR, partial response; SD, stable disease; MR, mixed response; PD, progressive disease; NA, not assessed.

(C) Age and sex distribution.

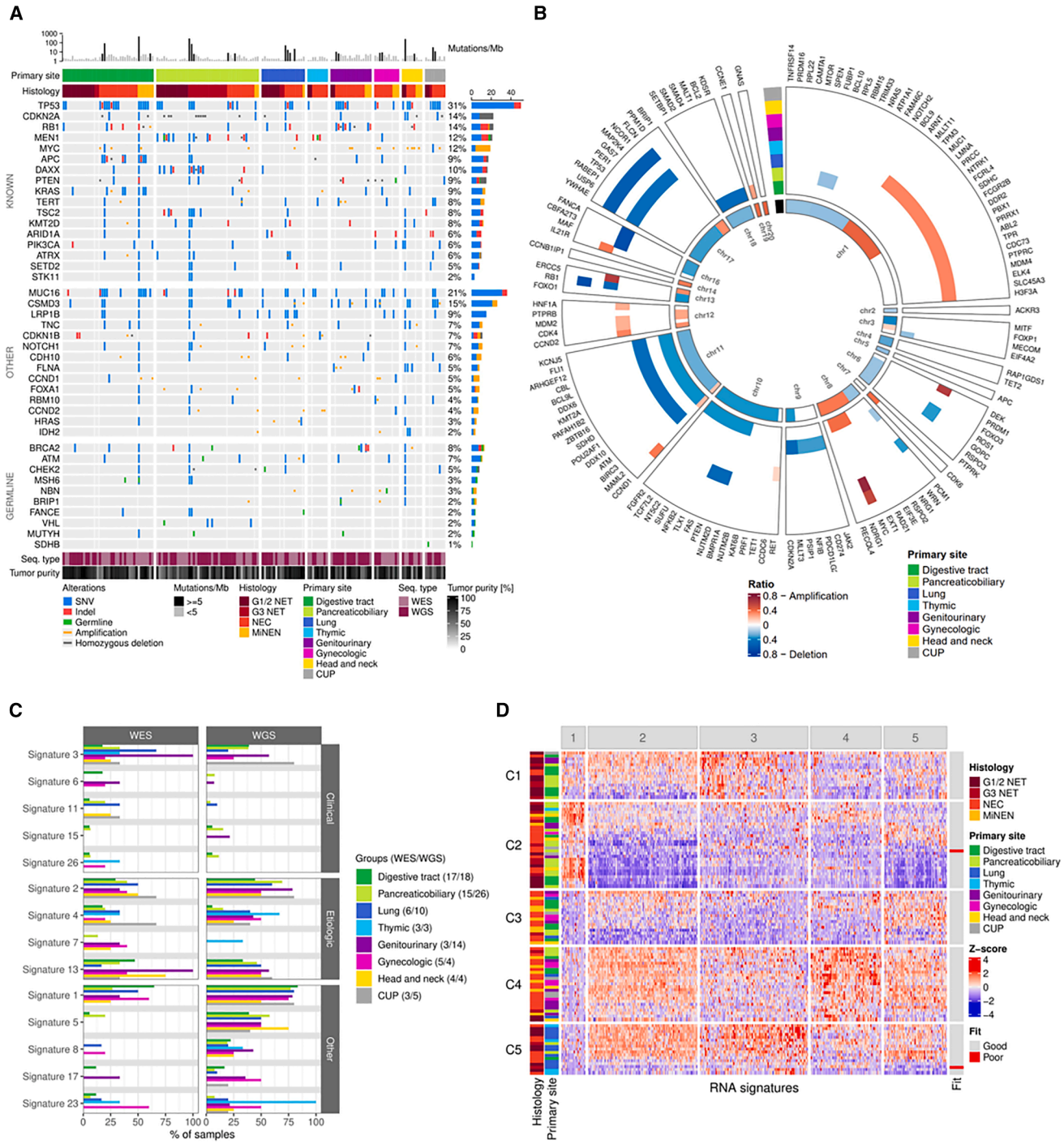

Figure 2. Genomic and transcriptomic landscape

(A) OncoPrint summarizing three gene groups genes: (1) cancer-related genes that exceed an alteration frequency of 15% (SNVs, small indels, amplifications, or homozygous deletions) in the full cohort or in at least one topologic subset (OTHER; hypermutated samples excluded from frequency calculation), (2) established NEN driver genes (KNOWN), and (3) genes associated with hereditary tumor predisposition syndromes (GERMLINE). Each column corresponds to an individual patient, and each row represents a gene. Patients are ordered by primary tumor site, then by histologic subtype. The bar plot above the heatmap shows the total number of somatic mutations per patient, with black bars highlighting cases with an elevated TMB. Annotations below the heatmap denote the DNA sequencing modality (purple) and estimated tumor purity (gray). Gene-level alteration frequencies across the cohort are shown to the right of the heatmap.

(B) Significantly amplified or deleted cancer-related genes by primary site. Genes are arranged by genomic location, with copy-number gains in red and losses in blue. The intensity of red and blue indicates the proportion of samples within each primary site group that harbors the alteration. chr, chromosome.

(legend continued on next page)

patients, 31.2%; Figure 2A). *TP53* alteration rates varied by subtype: 42.7% in NECs, 36.8% in MiNENs, 18.2% in G3 NETs, and 15.9% in G1/2 NETs (Figures 2A and S1B). The frequency of *TP53* alterations also varied substantially between histology and localization combinations, occurring in 71.4% of gastrointestinal MiNENs and 66.7% NECs of unknown primary site but none observed in thymic NECs. Other known NEN drivers also showed subtype- and site-specific patterns. For instance, *MEN1* and *DAXX* mutations were enriched in pancreaticobiliary NETs, occurring in 35.7% ($p = 0.0176$) and 28.6% ($p = 0.036$), respectively, of G1/2 tumors and in 29.4% ($p = 0.042$) and 41.2% ($p = 0.00028$), respectively, of G3 tumors. Unlike *DAXX*, *MEN1* was also mutated in 33.3% of pancreaticobiliary NECs ($p = 0.046$). *VHL* alterations were exclusively observed in pancreaticobiliary NENs ($p = 0.006$). *APC* and *KRAS* alterations were more frequent in digestive high-grade NENs of the digestive tract: *APC* mutations were detected in 35.3% of gastrointestinal NECs ($p = 0.002$) and 57.1% of gastrointestinal MiNENs ($p = 0.003$), while *KRAS* mutations occurred in 23.5% of gastrointestinal NECs ($p = 0.045$) and 42.9% of gastrointestinal MiNENs ($p = 0.047$). *MYC* amplifications were predominantly observed in NECs and MiNENs of the head and neck ($p = 0.002$ for NECs and MiNENs vs. all others; Figure S1B). Other known driver genes, including *CDKN2A* (13.8%), *PTEN* (8.8%), *BRCA2* (7.5%), *TSC2* (7.5%), and *PIK3CA* (6.3%), were altered at lower frequencies. *TERT* mutations were predominantly detected in NECs (14.7%, $p = 0.001$; Figures 2A and S1B). We also identified alterations of uncertain oncogenic relevance in genes not previously implicated in NENs, such as *MUC16* (20.6%), *CSMD3* (15%), *AKAP9* (10.6%), and *LRP1B* (9.4%). *MUC16* alterations were significantly enriched in MiNENs (42.1%, $p = 0.029$), particularly in gastrointestinal MiNENs (71.4%, $p = 0.004$). *CSMD3* alterations were most frequent in NECs of unknown primary site (66.7%, $p = 0.005$), while *LRP1B* alterations were found in 26.3% of lung NENs ($p = 0.019$; Figures 2A and S1B).

We also observed a broad spectrum of somatic copy-number alterations (sCNAs) across various histologic and anatomic subgroups (Figures 2B and S1C). Across the entire cohort, frequent copy-number gains occurred on chromosomes 1q, 8q (*MYC*), 11q (*CCND1*), 12q (*MDM2*), 14p, 17q, 19q (*CCNE1* and *AKT2*), and 20q (*GNAS*). Some morphologic subtype-specific copy-number gains were strongly enriched in NECs (broad amplifications on 1q, 8q, 13q, 14p, 17q, and 19q) and/or MiNENs (more focal gains encompassing *MYC*, *CCND1*, and *MDM2*; Figure S1C). Gains on chromosomes 1 and 12q (the latter encompassing *CDK4*, *MDM2*, and *CCND2*) mainly occurred in thymic NENs. Focal chromosome 8 gains spanning the *MYC* locus were enriched in gynecologic and head and neck NENs, while broader amplifications involving *MYC* were seen in gastrointestinal NENs (Figure 2B). Narrow amplifications on chromosome 6 involving *DEK* were frequently observed in genitourinary NENs. Across the entire cohort, frequent copy-number losses occurred on chromosomes 1p (*CAMTA1* and *FAM46C*), 3p (*MITF* and *FOXP1*), 4q (*TET2*), 5q (*APC*), 6q, 8p (*NRG1* and *WRN*), 9p (*CDKN2A*), 10q (*PTEN*), 11q (*ATM*), 13q (*BRCA2*), 16q (*FANCA*), 17p (*TP53* and *MAP2K4*), and 18q (*SMAD2* and *SMAD4*). The established tumor suppressors *MEN1*, *ATRX*, and *DAXX* were affected by deletions in 17.9%, 12.8%, and 5.1% of cases, respectively. Subtype-enriched copy-number losses involved chromosomes 1p and 8p (*WRN* and *NRG1*) in NECs and MiNENs; 10q (*PTEN*) in G1/2 NETs, NECs, and MiNENs; 13q (*RB1*, *FOXO1*, and *BRCA2*) in NECs; 17p (*TP53* and *MAP2K4*) in NECs and MiNENs; 18q (*SMAD4*) in NECs and MiNENs; and 22q (*SMARCB1*) in MiNENs (Figure S1C). Tumor-site-enriched losses included chromosome 10q (*PTEN*) in genitourinary and digestive tract NENs, 9p (*CDKN2A*) in pancreaticobiliary NENs, and 13q (*RB1*) in genitourinary NENs (Figure 2B). Finally, homologous recombination deficiency (HRD) scores indicated significantly higher genomic instability in NECs and MiNENs than in G1/2 or G3 NETs (Figure S1D).

We also assessed single-base substitution mutational signatures (SBSs),[28] focusing on 14 clinically relevant or etiologically defined patterns as well as those frequently observed in our cohort. These analyses were stratified by sequencing method (WGS vs. WES; Figure 2C). SBS3, associated with HRD, was present across the entire cohort (Figures 2C and S1E). In four of 21 TMB-high cases, we detected SBS6 ($n = 3$), SBS15 ($n = 3$), or SBS26 ($n = 1$), all associated with defective DNA mismatch repair (MMR) (Figures 2C and S2E). Notably, SBS11, linked to prior temozolomide exposure, was observed in 10 NEN cases. SBS4, associated with tobacco smoking, emerged predominantly in high-grade NENs. SBS2 and SBS13, correlated with increased APOBEC cytidine deaminase activity, occurred concurrently but at low frequency throughout the cohort. In one of two patients carrying heterozygous germline *MUTYH* alterations, we detected SBS18 linked to mutant *MUTYH*, previously reported in pancreatic NETs.[13] Additionally, several signatures of unknown etiology were identified in various NEN subgroups (Figures 2C and S2E).

Using unsupervised classification of the entire cohort's RNA expression profiles, we identified five distinct transcriptional subtypes (Figure 2D). This analysis revealed tissue-specific patterns, including a cluster enriched for lung and thymic NENs (C5). Moreover, NETs, regardless of tissue origin, grouped together (C1 and C2), while MiNENs were numerically enriched in C3 and C4 (Figure 2D). Despite these discernible patterns, expression profiles were highly diverse, reflecting variations in primary site, histopathologic subtype, and possibly other, as-yet unidentified biological factors.

MTB recommendations

Our primary objective was to guide clinical decision-making through comprehensive molecular profiling. Therefore, a multidisciplinary MTB discussed 160 cases, delivering actionable recommendations for 146 patients (91.3%; Figures 1A and 3A). In two cases (1.3%), the detection of pathognomonic

(C) Clinically or etiologically relevant mutational signatures, grouped by primary tumor site. The plots display the proportion of samples with each signature in different NEN subcohorts.

(D) Unsupervised clustering of RNA-seq data, identifying five robust clusters (C1–C5) based on RNA expression patterns. A sample's adherence (fit) to its assigned cluster is classified based on the silhouette score.

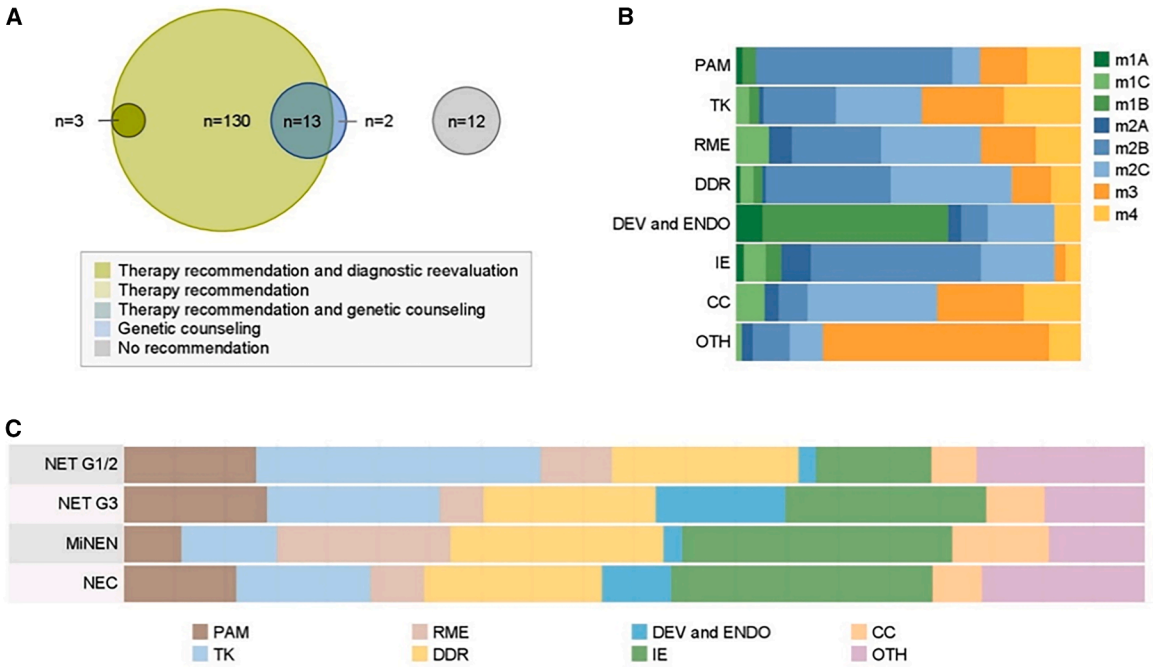

Figure 3. Overview of MTB recommendations

(A) Numbers and distribution of patients with therapeutic, diagnostic, and genetic counseling recommendations.

(B) Relative distribution of DKFZ/NCT/DKTK molecular evidence levels of MTB recommendations in the different treatment baskets. OTH, other.

(C) Relative frequency of recommendations from the different treatment baskets according to histopathologic subtype.

molecular alterations followed by histopathologic reassessment led to revised diagnoses of non-NEN malignancies, i.e., desmoplastic small round cell tumor (*EWSR1::WT1* fusion) and Ewing sarcoma (*EWSR1::FLI1* fusion). In 15 patients (9.4%), pathogenic germline findings prompted genetic counseling (Figure 3A); in 11 of these, previously unrecognized hereditary cancer syndromes associated with NEN were diagnosed. In 144 patients (90%), the MTB provided at least one molecularly guided treatment recommendation. These recommendations were classified according to an evidence framework established in MASTER and other German precision oncology initiatives, including the National Network for Genomic Medicine and the German Network for Precision Medicine. Recommended systemic therapies were categorized into eight treatment "baskets," reflecting core biological mechanisms targeted by available drugs (Figure 3B). Among these categories, the developmental pathways and endocrine signaling (DEV and ENDO) basket had the highest proportion of recommendations with clinical evidence levels, mainly due to therapies targeting somatostatin receptor (SSTR) family members, followed by the immune evasion (IE), DNA damage repair (DDR), and RAS/RAF/MEK/ERK signaling (RME) baskets. Drugs from the PI3K/AKT/mTOR signaling (PAM; i.e., everolimus) and tyrosine kinase signaling (TK; i.e., sunitinib) baskets typically had lower evidence levels and could often not be recommended because patients had already received them as part of standard-of-care treatment and had developed resistance before predictive biomarkers were detected. The limited clinical evidence for these drugs in NENs reflects the scarcity of molecularly stratified clinical trials in this field. Consequently, many recommendations relied on evidence extrapolated from other tumor types or preclinical studies (DKFZ/NCT/DKTK evidence levels m2 and m3, respectively; Figure 3B).

A detailed analysis of treatment decisions by morphologic subgroup (Figure 3C) showed that most recommendations were issued for drugs from the IE basket, followed by DDR- and TK-directed therapies. Within the IE category, immune checkpoint inhibitors and antibody-drug conjugates were more frequently recommended for NECs and MiNENs than for G1/2 and G3 NETs (56% and 62% vs. 28% and 45%, respectively). DDR-targeted therapies included PARP inhibitors, their combination with conventional cytotoxic agents, and platinum-based chemotherapy regimens. Fewer recommendations fell into the cell cycle (CC) basket, reflecting the low prevalence and uncertain clinical relevance of associated predictive biomarkers in NENs. Recommendations from the TK basket, comprising FGFR, ERBB, RET, ALK, JAK2, and VEGFR inhibitors, were relatively more common in G1/G2 NETs than in NECs (60% vs. 37%) and MiNENs. Together, these data show that WGS/WES and RNA-seq yield molecularly guided treatment recommendations for a substantial proportion of heavily pretreated patients with advanced NENs across all subtypes.

Biomarkers underlying MTB recommendations

The number of recurrent biomarkers used across different treatment baskets ranged from five to 22, with many recommendations supported by multiple biomarkers (median, 2; range, 1–18). The DDR basket encompassed the most biomarkers due

to the large number of DNA repair genes and complex biomarkers indicative of HRD, including (1) SBS3; (2) genomic instability metrics, i.e., loss-of-heterozygosity score, number of large-scale state transitions, and extent of telomeric allelic imbalance; and (3) somatic and germline alterations in HRD-associated genes. For example, we detected oncogenic SNVs and small indels in established DDR genes such as *BRCA2* and *ATM* in a large subset of NEN cases (Figure 4A). Both single-gene and complex HRD biomarkers were identified across all histopathologic subtypes, an observation not previously described in advanced NENs.

Biomarkers in the PAM basket encompassed alterations in *PTEN*, *PIK3CA*, *VHL*, and *TSC1*; the CC basket mainly comprised *CDKN2A* mutations or deletions; and the RME basket included alterations in *NF1*, *NF2*, *KRAS*, *HRAS*, and *BRAF* (Figure 4A). Within the TK basket, RNA-based biomarkers were particularly common, specifically overexpression of *FGFR*, *VEGFR*, and *ERBB* family members and their corresponding ligands. Biomarkers in the IE basket included alterations in single genes, e.g., loss-of-function *MSH2* mutations, elevated *CTLA4* or *MAGEA3* expression, high TMB, and specific mutational signatures such as SBS2 (Figure 4A). Recommendations for SSTR-directed therapy were based on increased RNA expression of *SSTR* family members in NECs, G3 NETs, and, in rare instances, previously untreated G1 NETs (Figure 4B). Validation of SSTR expression by positron emission tomography (PET) imaging was initiated in these cases.

To maximize the identification of potential therapeutic intervention points, we also analyzed the expression of structurally intact genes encoding proteins targetable by antibodies, antibody-drug conjugates, cellular immunotherapies, or therapeutic vaccines. Our analysis revealed several candidates with distinct expression patterns: some were specific to the tissue of origin, e.g., *CDH17*, while others reflected neuroendocrine differentiation, e.g., *DLL3*, and we also identified novel targets, such as *PRAME* in MiNENs and *MAGEA1* in pancreatic NENs (Figures 4B and S2).

As many patients had multiple actionable biomarkers, the MTB often provided several treatment recommendations per case (median, 3; range, 0–8). Nearly half of these (47%) included drug combinations, most of which were already established in other cancer types with well-documented toxicity profiles. Common examples included dual immune checkpoint blockade (e.g., ipilimumab plus nivolumab), BRAF and MEK inhibitors (e.g., dabrafenib plus trametinib), and chemotherapy combined with PARP inhibition (e.g., trabectedin plus olaparib).

Response to MTB-guided therapies

To evaluate the clinical impact of molecularly guided treatment decisions, we analyzed outcomes in 57 patients who collectively received 85 therapies recommended by the MTB; response assessments were available for 45 patients and 68 therapies. Most treatments administered consisted of immune checkpoint inhibitors, kinase inhibitors, or HRD-directed therapies, discussed in more detail below. Among the 68 evaluable therapies, 47 (69.1%) demonstrated clinical benefit, including 25 PRs and 22 cases of stable disease (SD). At the patient level, 34 of 57 (59.6%) derived clinical benefit from at least one therapy, with 18 achieving PRs and 16 SD as their best outcome, including cases with multiple qualifying responses. Kaplan-Meier analysis showed a non-significant trend toward improved overall survival in patients receiving MTB-recommended therapies (Figure S3A), driven by a statistically significant benefit in the NEC and MiNEN subcohorts (log rank test, $p = 0.025$; Figure S3B). No significant difference in survival was observed in patients with NETs (Figure S3C). Table S3 summarizes all implemented MTB-recommended therapies.

Immune checkpoint blockade

Recent clinical trials evaluating immune checkpoint blockade, with or without temozolomide, have demonstrated encouraging overall response rates of 32%–44% in NENs.[29–33] While the roles of viral integration and ultraviolet-induced mutations in Merkel cell carcinoma are well established,[34] emerging evidence suggests that microsatellite instability (MSI) and high TMB may predict response, particularly in high-grade NENs. In our cohort, 20 patients received a total of 24 MTB-recommended immune checkpoint inhibitor therapies, including 11 with NECs, three with G3 NETs, four with MiNENs, and two with G1/2 NETs (Figure 5A; Table S3). Four patients exhibited very high TMB, consistent with MSI (Figure 5A). However, only one patient, who had a pathogenic germline variant in *MSH6*, showed a definitive MSI marker in the tumor, i.e., an elevated MSI score. Somatic hypermutation has been sporadically observed in NENs and can, in some cases, arise after temozolomide treatment[35–37] through adaptive downregulation of the DNA MMR pathway, typically via mutations in MMR genes.[38] This temozolomide-associated deficient MMR phenotype mirrors MSI arising independently of temozolomide exposure and may similarly confer vulnerability to immune checkpoint inhibition.

Indeed, the other three patients with very high TMB had temozolomide-pretreated tumors that displayed the characteristic alkylator-associated SBS11 (C-to-T substitutions accounting for more than 90% of SNVs), accompanied by a smaller fraction of SBS15, associated with defective DNA MMR, and somatic alterations in *MSH2* and *MSH6* (Figure 5B). All three patients experienced durable responses to immune checkpoint blockade (for details on two cases, see Figures S4A and S4B). Among the 47 temozolomide-pretreated patients in our cohort, seven (14.9%) displayed SBS11; four of these had a TMB exceeding 5 mut/Mb. Notably, a subsequent biopsy from pat-090, taken after progression on combination immune checkpoint inhibition, no longer exhibited SBS11 and showed a substantially lower TMB (9.3 mut/Mb), consistent with clonal selection. These findings highlight that temozolomide can induce MMR deficiency and, consequently, a high TMB, sensitizing a relevant fraction of patients with NENs to immune checkpoint blockade (Figure 5B).

Kinase inhibition

Currently, sunitinib and cabozantinib are the only multitargeted tyrosine kinase inhibitors approved by the United States Food and Drug Administration for the treatment of NENs, specifically well-differentiated tumors, and further compounds, such as lenvatinib, axitinib, and surufatinib, have shown activity. However, there is limited evidence regarding predictive molecular biomarkers for their use. To address this gap, our MTB recommended kinase inhibitors for 18 patients with non-pancreatic and/or

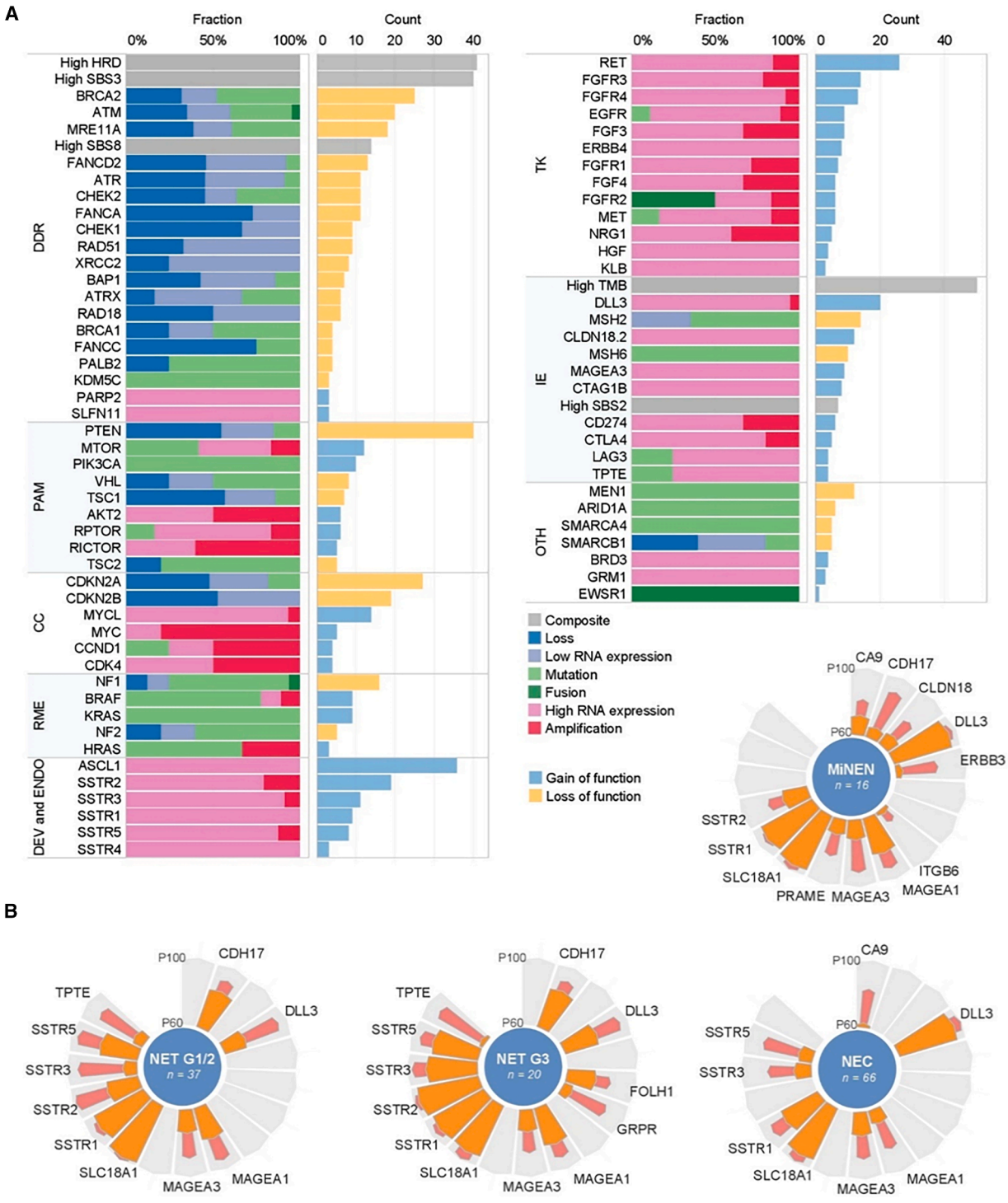

Figure 4. Clinically actionable biomarkers

(A) Overview of single-gene and composite molecular biomarkers that were assigned to treatment baskets, ranked by their frequency of supporting MTB recommendations. The left image depicts the relative distribution of biomarker categories and alteration types across treatment baskets. The right image shows the corresponding absolute counts for each biomarker along with functional annotations relevant to therapy selection.

(B) RNA expression of established and emerging therapeutic targets in different NEN subtypes. Colored symbols indicate the percentage of NENs expressing a given gene above the 50th (orange) and 75th (red) percentiles, defined by a reference cohort of 1,207 non-NEN cancers.

A

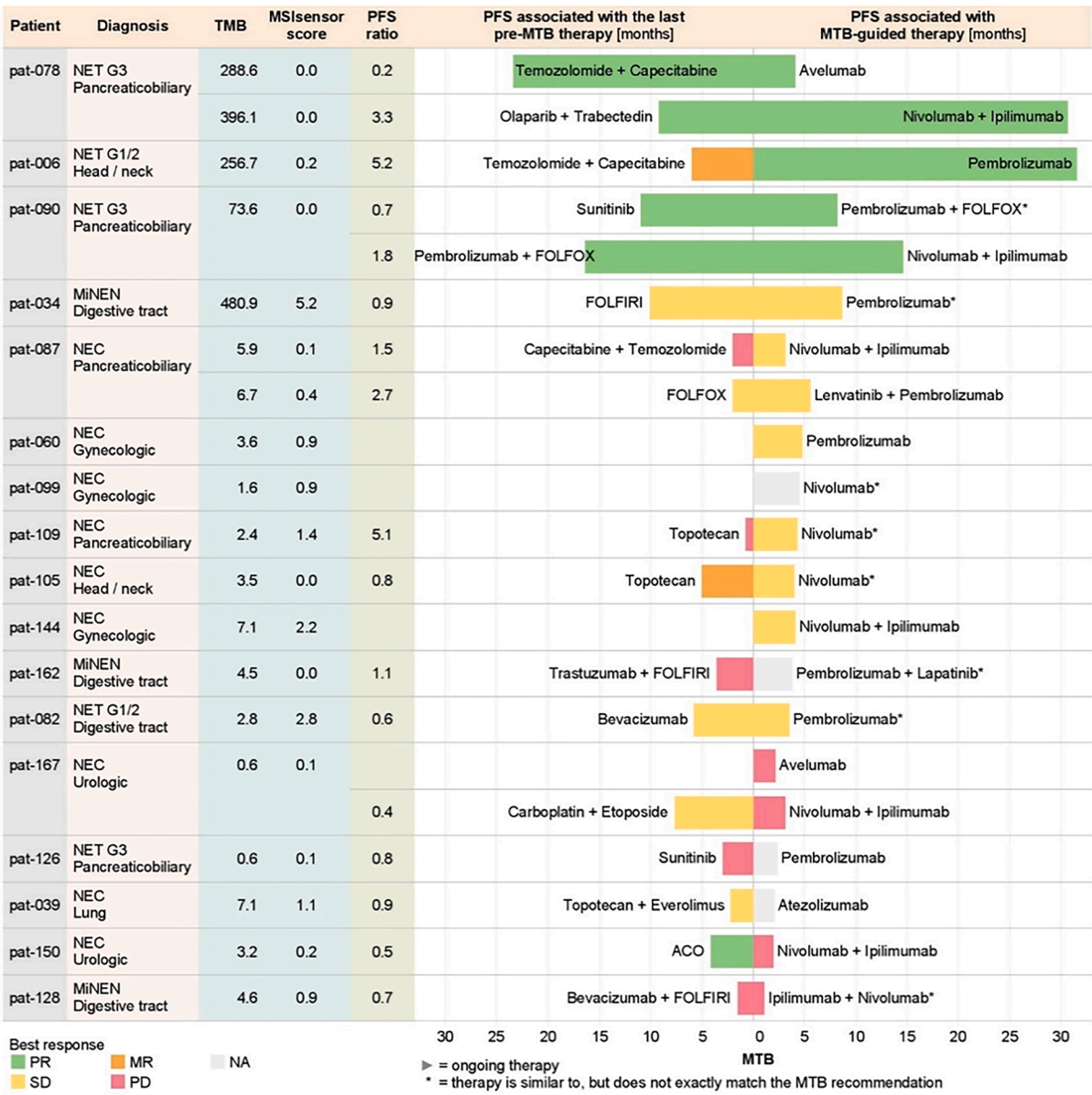

B

Patient	Biomarker	Before temozolomide therapy	Temozolomide therapy	After temozolomide therapy	After progression to checkpoint inhibitor therapy
pat-006	SBS11	0%	21 months	87%	NA
	TMB [mut/MB]	0.6		256.7	NA
pat-078	SBS11	NA	23 months	100%	NA
	TMB [mut/MB]	3.13		288.6	NA
pat-090	SBS11	NA	3 months	78%	0%
	TMB [mut/MB]	NA		73.6	9.3

Figure 5. Molecularly guided immune checkpoint inhibitor therapies

(A) Clinical benefit from molecularly guided immune checkpoint inhibitor therapies. TMB (mutations per megabase) and MSI scores for each case are shown. Bars depict the best response and progression-free survival (PFS) achieved with the treatment administered prior to MTB evaluation and with the therapy recommended by the MTB. ACO, adriamycin, cyclophosphamide, vincristine; FOLFIRI, folinic acid, 5-fluorouracil, irinotecan; FOLFOX, folinic acid, 5-fluorouracil, oxaliplatin.
(B) SBS11 and TMB before and after temozolomide treatment and after immune checkpoint inhibition in three patients with NENs.

Patient	Diagnosis	Biomarkers	MTB recommendation	PFS ratio	PFS associated with the last pre-MTB therapy [months]	PFS associated with MTB-guided therapy [months]
pat-113	NET G1/2 CUP	MET T1010I	MET inhibitor	3.8	FOLFOX	Cabozantinib
pat-091	NET G3 Digestive tract	FGFR3 amplification; FGFR3, RET high expression	FGFR, RET inhibitor	1.4	Octreotide + Everolimus	Sunitinib
pat-065	NET G3 Pancreaticobiliary	VEGFA, FLT1, KDR, FLT4 high expression; VHL D143E	VEGFR inhibitor	0.9	Streptozotocin + 5-FU	Sunitinib
pat-056	NET G3 Pancreaticobiliary	BRAF V600E	BRAF inhibitor + MEK inhibitor	2.9	Avelumab	Trametinib + Dabrafenib
		BRAF V600E + intron 1-8 deletion	Encorafenib + Binimetinib	3.1	Carboplatin + Etoposide	Encorafenib + Binimetinib
pat-098	NEC Digestive tract	BRAF V600E	BRAF inhibitor + MEK inhibitor	2.6	Cisplatin + Etoposide	Trametinib + Dabrafenib
pat-104	NEC CUP	KIT V560D; KIT, FGFR3 high expression	KIT, FGFR inhibitor	0.7	FOLFOX	Sunitinib
				5.9	Avelumab	Paclitaxel + Ponatinib
				0.4	FOLFIRI	Avapritinib
pat-042	NET G1/2 Lung	FGFR2, FGFR3, FGFR4 high expression	FGFR inhibitor	0.7	Temozolomide	Nintedanib
pat-050	NET G1/2 Lung	FGFR3::TACC2; KDM5C E646V; RET high expression	FGFR, RET inhibitor	1.1	Everolimus	Sunitinib
pat-126	NET G3 Pancreaticobiliary	RET high expression	RET inhibitor	0.9	FOLFIRI	Sunitinib*
pat-055	NET G1/2 Digestive tract	FGFR4 high expression	FGFR inhibitor	0.7	Vandetanib	Pazopanib
				0.4	Lanreotide	Vandetanib
pat-143	NET G3 Pancreaticobiliary	FGF3, FGF4, FGFR1 high expression	FGFR inhibitor	1.0	Everolimus	Lenvatinib
pat-063	NEC Digestive tract	MET amplification; HGF, MET high expression	MET inhibitor	0.5	FOLFIRI	Crizotinib
pat-116	NET G3 Digestive tract	EWSR1::ATF1; ALK high expression	ALK inhibitor	0.5	Pazopanib	Pazopanib + Crizotinib*
				0.9	Pazopanib + Crizotinib	Alectenib
pat-023	NEC Digestive tract	FGF3, FGF4, FGFR3, FGFR4 high expression	FGFR inhibitor	0.2	FOLFOX	Ponatinib
pat-127	NET G1/2 Thymus	ASCL1, FGFR3 high expression	FGFR inhibitor			Ponatinib
pat-141	NET G3 Pancreaticobiliary	FGF3 high expression	FGFR inhibitor	0.2	Everolimus	Sunitinib

Figure 6. Molecularly guided kinase inhibitor therapies

Individual biomarkers and the corresponding MTB-recommended therapies are shown for each case. Bars depict the best response and PFS achieved with the treatment administered prior to MTB evaluation and with the therapy recommended by the MTB. FOLFIRI, folinic acid, 5-fluorouracil, irinotecan; FOLFOX, folinic acid, 5-fluorouracil, oxaliplatin.

high-grade NENs (Figure 6; Table S3), including two cases where they were combined with immune checkpoint blockade. In 10 cases, this was guided by mRNA (over)expression of *VEGFR*, *FGFR*, and *RET*. Among those with evaluable outcomes, two had PRs, two achieved SD, and three experienced disease progression. Two additional recommendations for tyrosine kinase inhibitors targeting ALK and MET overexpression did not yield disease control. Beyond expression-based biomarkers, we identified rare genomic alterations warranting kinase inhibitor therapy, including *FGFR3* fusions and a single SNV in MET. Moreover, three patients received kinase inhibitor therapy recommendations based on well-characterized actionable mutations, i.e., BRAF p.V600E[39,40] and KIT p.V560D (Figure 6; Table S3). Two of these cases, which showed exceptional responses, are presented in detail in the supplemental information (Figure S5).

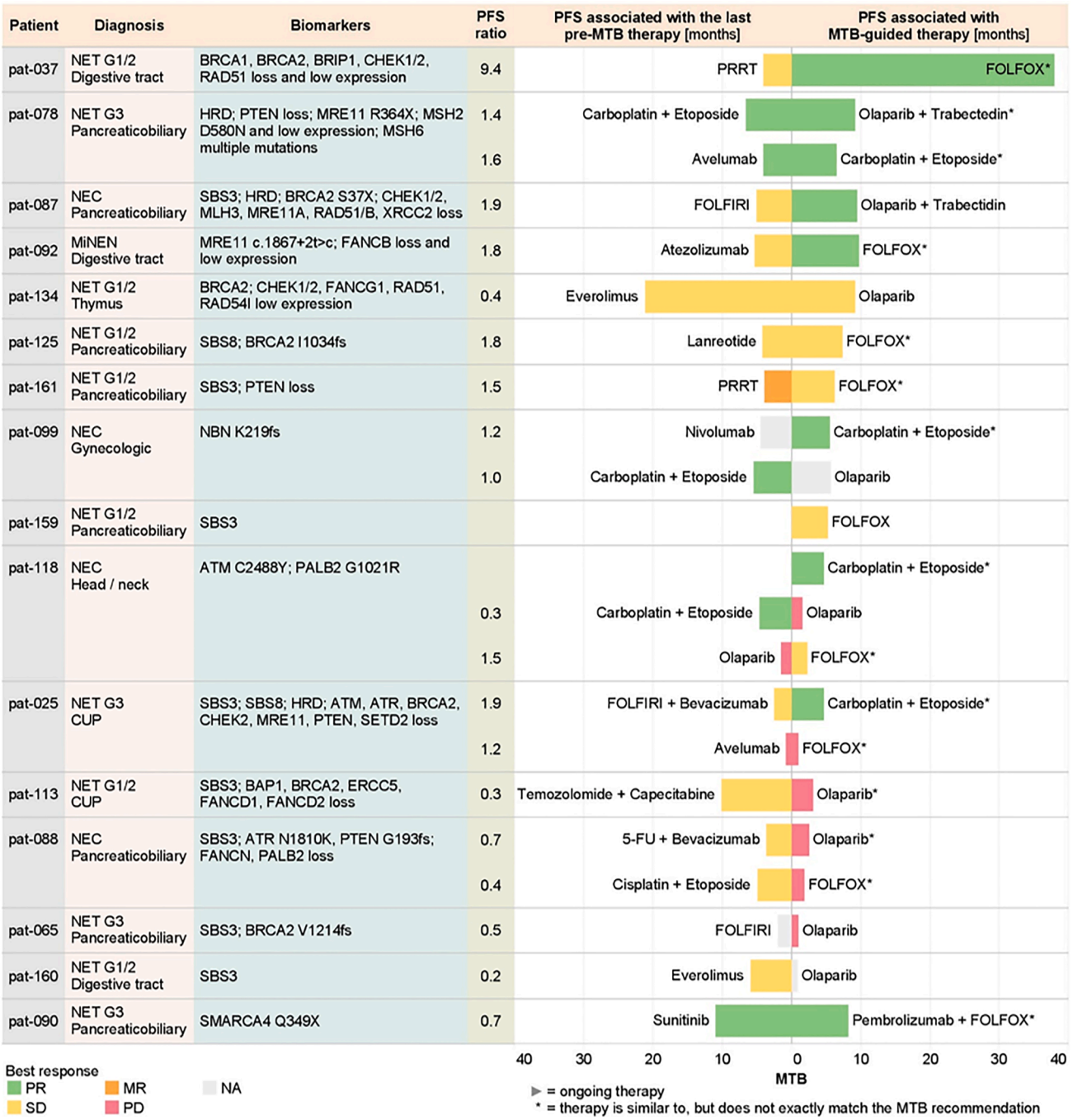

Figure 7. Molecularly guided PARP inhibitor or platinum-based therapies

Individual biomarkers supporting PARP inhibitors and/or platinum-based therapy recommendations are shown for each case. Bars depict the best response and PFS achieved with the treatment administered prior to MTB evaluation and with the treatment administered after the MTB and following a MTB recommendation. FOLFIRI, folinic acid, 5-fluorouracil, irinotecan; FOLFOX, folinic acid, 5-fluorouracil, oxaliplatin; PRRT, peptide receptor radiotherapy.

PARP inhibition

PARP inhibitors exploit synthetic lethality arising from HRD, a recognized hallmark of certain malignancies, particularly ovarian cancer. HRD and its corresponding mutational signatures, such as SBS3, have emerged as biomarkers predicting response to PARP inhibitors and platinum-based therapies in various tumor types.[41,42] Given the frequent sensitivity of high-grade NETs and NECs to platinum compounds, we investigated the potential efficacy of PARP inhibitors and/or platinum-based chemotherapies in NENs and whether genomic biomarkers of HRD could guide their clinical use. Among 10 patients treated with PARP inhibitors based on genomic profiling,

two achieved PRs, both occurring in high-grade pancreatic NENs (Figure 7). Notably, these responses were observed only when PARP inhibitors were combined with trabectedin, despite prior exposure to platinum-based therapies, suggesting a possible synergistic interaction. Consistent with these clinical observations, high HRD scores and/or the presence of SBS3 were detected in many NENs, with NECs and MiNENs showing significantly higher HRD scores (Figures 2C and S1D). Although eight of 21 patients derived clinical benefit from HRD-targeted treatments (Figures 7 and S4A; Table S3), no significant differences in HRD-associated biomarkers distinguished responders from non-responders among patients who received PARP inhibitors or platinum-based therapies per MTB recommendations. Neither SBS3, HRD scores, nor mutations in HRD-related genes showed a predictive association with response to targeted therapies in our cohort.

DISCUSSION

Previous studies have provided insights into the molecular landscape of NENs.[13,43,44] However, the clinical implications of molecular analyses in these tumors have only recently begun to emerge. In this study, we investigated the utility of genomic and transcriptomic profiling in 160 patients with advanced, extensively pretreated NENs enrolled in the NCT/DKTK/DKFZ MASTER program, a prospective registry trial focused on rare cancers. We observed substantial molecular heterogeneity, likely reflecting both the diverse cellular origins of NENs and varying treatment histories that potentially promote tumor evolution through selective pressure. Furthermore, our analysis of real-world clinical outcomes in 57 patients with NENs receiving molecularly guided therapies provided insights into the impact of precision oncology approaches in this challenging disease context. The implementation rate of molecularly informed therapies and the clinical benefit observed in our cohort, particularly among patients with NECs and MiNENs, are broadly consistent with findings from other NEN studies. Notably, a study conducted at Institut Gustave Roussy involving 114 patients with diverse NENs who underwent panel-based sequencing supplemented with TMB and MSI assessment identified actionable alterations in 48% of cases; of the 19 patients who received matched therapies, 84% achieved disease control.[21] Although the disease control rate among patients receiving molecularly informed treatment was slightly lower in our study, the use of comprehensive molecular profiling enabled a higher rate of treatment recommendations and allowed the identification of complex predictive biomarkers for platinum-based therapies and PARP inhibitors. Additional studies similarly reported actionable biomarkers but provided limited information on downstream implementation and clinical outcomes. For example, van Riet et al. identified actionable alterations in 49% of patients, and Miyazawa et al. reported actionable biomarkers in 36% of cases, with an implementation rate of 14%, including two responses to immune checkpoint inhibitors.[43,45]

Our analysis reveals critical insights for individualized clinical management of patients with advanced-stage NENs. For example, patients with a high TMB following temozolomide therapy—comprising over 10% of temozolomide-pretreated patients in our cohort—demonstrated exceptional responses to subsequent immune checkpoint blockade.[35–37] Conversely, prior platinum-based chemotherapy in patients with HRD-associated tumors may have contributed to the suboptimal outcomes observed with PARP inhibitor monotherapy. These findings raise the fundamental question of when comprehensive molecular profiling should ideally be performed in patients with NENs. Early-stage analyses may allow for the detection of rare but actionable biomarkers, such as *BRAF* mutations, at a time when implementing targeted interventions could be most effective. Alternatively, profiling at disease progression may reveal novel therapeutic vulnerabilities emerging from tumor evolution beyond established clinical guidelines. While many known biomarkers can be detected through targeted gene panels,[21,46] only comprehensive profiling using WGS and RNA-seq can uncover novel therapeutic targets and resistance mechanisms. We identified several rare, previously unrecognized biomarkers in NENs that can be readily assessed using gene-panel-based assays (Table S4). However, to fully leverage the potential of multi-layered tumor profiling to guide clinical management in this challenging patient population, our study underscores the feasibility and added value of comprehensive molecular characterization using WGS and RNA-seq, which may be complemented by epigenomic and (phospho)proteomic analyses in the near future.

Our findings also establish a foundation for biomarker development and patient stratification in prospective clinical trials, potentially achieving meaningful clinical impact earlier in the disease course. We identified several mRNA-based biomarkers in advanced NENs that are promising candidates for inclusion in ongoing trials exploring antibody-drug conjugates or engineered autologous T cell therapies. Furthermore, comprehensive molecular profiling, such as WGS, harbors substantial untapped potential for detecting complex genomic biomarkers, including mutational signatures and compound scores derived from the integration of multiple molecular features. Such next-generation biomarkers, which frequently evade detection by conventional panel-based methods, create new opportunities for translational and clinical NEN research. For example, composite biomarkers of HRD may hold significant potential to identify patients likely to benefit from PARP inhibitors and platinum-based therapies.

Limitations of the study

In our precision oncology program, most patients with NENs present with advanced, heavily pretreated disease; accordingly, the molecular landscape described here is not representative of primary, treatment-naive NENs. Nonetheless, this study comprises one of the largest comprehensively profiled NEN cohorts reported to date. Despite the overall cohort size, several subtype- and tissue-specific groups remain small, underscoring the need to validate our findings in larger, dedicated studies. More granular molecular stratification by tissue of origin, as well as in-depth sex-/gender-specific analysis, would have been desirable but was not feasible given the limited number of cases in many subgroups. In addition, treatment response assessments were performed in a real-world setting and were not uniformly standardized across participating centers. Given the substantial

heterogeneity in primary tumor sites, molecular alterations, and administered therapies, our molecular and clinical findings should be regarded as hypothesis generating.

We used a comprehensive diagnostic strategy that included WGS/WES, RNA-seq, and imaging-based assessment of SSTR expression. Additional molecular layers, such as proteomics,[47] microRNA profiling,[48] or tumor and host gut microbiome analyses,[49] may further refine therapeutic stratification in NENs.[50] Although such multi-omics approaches are currently feasible in specialized centers, the increasing availability of next-generation sequencing raises the prospect that biomarker-guided therapies for advanced NENs could become more widely used in routine clinical practice.

The rarity and heterogeneity of NENs limit the feasibility of traditional prospective trials designed to validate individual biomarkers' predictive value in large, homogeneous patient cohorts. As a result, future validation efforts will necessarily rely on real-world, data-driven observational studies.[51] Despite these challenges, we remain optimistic that innovative translational strategies leveraging multi-layered tumor profiling will continue to advance our understanding of NEN biology and, ultimately, enable the development of individualized therapeutic approaches for patients with these rare and challenging cancers.

RESOURCE AVAILABILITY

Lead contact

Requests for further information and resources should be directed to and will be fulfilled by the lead contact, Stefan Fröhling (stefan.froehling@nct-heidelberg.de).

Materials availability

This study did not generate new unique reagents, plasmids, or mouse lines.

Data and code availability

- The DNA and RNA sequencing data generated in this study are available via controlled access in the German Human Genome-Phenome Archive (GHGA) at https://data.ghga.de/study/GHGAS12079965883832. Further details, including the study's data access policy, can be found there.
- Bioinformatics analyses were performed using open-source software listed in the key resources table, with parameters detailed in the corresponding STAR methods subsections.
- Any additional information required to reanalyze the data reported in this work paper is available from the lead contact upon request.

ACKNOWLEDGMENTS

We thank the NCT Sample Processing Laboratory and the DKFZ Next Generation Sequencing and Omics IT and Data Management Core Facilities for technical support. The MASTER program is supported by the NCT Overarching Clinical Translational Trial Program, the NCT Heidelberg Molecular Precision Oncology Program, and DKTK.

AUTHOR CONTRIBUTIONS

S.K., L.A., P.H., H.G., and S.F. conceptualized the study. M.P., P.H., H.G., and S.F. supervised the study. S.K., L.A., M.O., C.E.H., C.H., A.M., M.-V.T., B.H., L.G., B.K., K.B., D.R., A.B.-M., E.R., K.P., C.G., M.L., D.T.R., H.J., U.-F.P., M.A., A.S., E.C.W., B.W., D.J., E.S., U.K., M.P., P.H., H.G., and S.F. collected the clinical and molecular data. S.K., M.O., B.B., K.P., S.U., and D.H. developed the analysis methodology. S.K., L.A., B.H., K.B., A.B.-M., E.R., N.H., L.K., D.H., P.H., and E.K.-H. curated the clinical and molecular data. S.K., M.O., E.K.-H., S.U., and P.H. conducted the formal analyses. S.K., M.O., P.H., and E.K.-H. visualized the results. S.K., L.A., M.O., E.K.-H., P.H., and S.F. wrote the primary draft, which was critically reviewed, edited, and approved by all co-authors. S.K. and M.O. have full access to all data.

DECLARATION OF INTERESTS

S.K. declares the following: consulting or advisory board membership with and honoraria from Roche; C.H. declares the following: consulting or advisory board membership with Boehringer Ingelheim, honoraria from Roche and Novartis, and research funding from Boehringer Ingelheim. P.H. declares the following: consulting or advisory board membership with and honoraria from Platomics. S.F. declares the following: consulting or advisory board membership with and travel or accommodation expenses from Illumina.

STAR★METHODS

Detailed methods are provided in the online version of this paper and include the following:

- KEY RESOURCES TABLE
- EXPERIMENTAL MODEL AND STUDY PARTICIPANT DETAILS
  - Patients
- METHOD DETAILS
  - Sample processing
  - DNA sequencing
  - Somatic SNV and indel calling
  - Germline SNV and indel calling
  - Somatic structural variant calling
  - Somatic CNA calling
  - TMB quantification
  - Mutational signature analysis
  - HRD scoring
  - MSI detection
  - RNA-seq and gene fusion detection
  - RNA-based clustering
- QUANTIFICATION AND STATISTICAL ANALYSIS
- ADDITIONAL RESOURCES

SUPPLEMENTAL INFORMATION

Supplemental information can be found online at https://doi.org/10.1016/j.medj.2026.101130.

Received: July 27, 2025
Revised: September 10, 2025
Accepted: April 6, 2026
Published: April 30, 2026

REFERENCES

1. Loree, J.M., Chan, D., Lim, J., Stuart, H., Fidelman, N., Koea, J., Posavad, J., Cummins, M., Doucette, S., Myrehaug, S., et al. (2024). Biomarkers to Inform Prognosis and Treatment for Unresectable or Metastatic GEP-NENs. JAMA Oncol. *10*, 1707–1720.
2. van der Graaf, W.T.A., Tesselaar, M.E.T., McVeigh, T.P., Oyen, W.J.G., and Fröhling, S. (2022). Biology-guided precision medicine in rare cancers: Lessons from sarcomas and neuroendocrine tumours. Semin. Cancer Biol. *84*, 228–241.
3. Kawasaki, K., Rekhtman, N., Quintanal-Villalonga, Á., and Rudin, C.M. (2023). Neuroendocrine neoplasms of the lung and gastrointestinal system: convergent biology and a path to better therapies. Nat. Rev. Clin. Oncol. *20*, 16–32.
4. Suehnholz, S.P., Nissan, M.H., Zhang, H., Kundra, R., Nandakumar, S., Lu, C., Carrero, S., Dhaneshwar, A., Fernandez, N., Xu, B.W., et al.

(2024). Quantifying the Expanding Landscape of Clinical Actionability for Patients with Cancer. Cancer Discov. *14*, 49–65.

5. Horak, P., Heining, C., Kreutzfeldt, S., Hutter, B., Mock, A., Hüllein, J., Fröhlich, M., Uhrig, S., Jahn, A., Rump, A., et al. (2021). Comprehensive Genomic and Transcriptomic Analysis for Guiding Therapeutic Decisions in Patients with Rare Cancers. Cancer Discov. *11*, 2780–2795.
6. Rindi, G., Mete, O., Uccella, S., Basturk, O., La Rosa, S., Brosens, L.A.A., Ezzat, S., de Herder, W.W., Klimstra, D.S., Papotti, M., and Asa, S.L. (2022). Overview of the 2022 WHO Classification of Neuroendocrine Neoplasms. Endocr. Pathol. *33*, 115–154.
7. Chandrasekharappa, S.C., Guru, S.C., Manickam, P., Olufemi, S.E., Collins, F.S., Emmert-Buck, M.R., Debelenko, L.V., Zhuang, Z., Lubensky, I.A., Liotta, L.A., et al. (1997). Positional cloning of the gene for multiple endocrine neoplasia-type 1. Science *276*, 404–407.
8. Jiao, Y., Shi, C., Edil, B.H., de Wilde, R.F., Klimstra, D.S., Maitra, A., Schulick, R.D., Tang, L.H., Wolfgang, C.L., Choti, M.A., et al. (2011). DAXX/ATRX, MEN1, and mTOR pathway genes are frequently altered in pancreatic neuroendocrine tumors. Science *331*, 1199–1203.
9. Banck, M.S., Kanwar, R., Kulkarni, A.A., Boora, G.K., Metge, F., Kipp, B.R., Zhang, L., Thorland, E.C., Minn, K.T., Tentu, R., et al. (2013). The genomic landscape of small intestine neuroendocrine tumors. J. Clin. Investig. *123*, 2502–2508.
10. Fernandez-Cuesta, L., Peifer, M., Lu, X., Sun, R., Ozretić, L., Seidal, D., Zander, T., Leenders, F., George, J., Müller, C., et al. (2014). Frequent mutations in chromatin-remodelling genes in pulmonary carcinoids. Nat. Commun. *5*, 3518.
11. Francis, J.M., Kiezun, A., Ramos, A.H., Serra, S., Pedamallu, C.S., Qian, Z.R., Banck, M.S., Kanwar, R., Kulkarni, A.A., Karpathakis, A., et al. (2013). Somatic mutation of CDKN1B in small intestine neuroendocrine tumors. Nat. Genet. *45*, 1483–1486.
12. Neou, M., Villa, C., Armignacco, R., Jouinot, A., Raffin-Sanson, M.-L., Septier, A., Letourneur, F., Diry, S., Diedisheim, M., Izac, B., et al. (2020). Pangenomic Classification of Pituitary Neuroendocrine Tumors. Cancer Cell *37*, 123–134.e5.
13. Scarpa, A., Chang, D.K., Nones, K., Corbo, V., Patch, A.-M., Bailey, P., Lawlor, R.T., Johns, A.L., Miller, D.K., Mafficini, A., et al. (2017). Whole-genome landscape of pancreatic neuroendocrine tumours. Nature *543*, 65–71.
14. Kasajima, A., Konukiewitz, B., Schlitter, A.M., Weichert, W., and Klöppel, G. (2022). An analysis of 130 neuroendocrine tumors G3 regarding prevalence, origin, metastasis, and diagnostic features. Virchows Arch. *480*, 359–368.
15. Venizelos, A., Elvebakken, H., Perren, A., Nikolaienko, O., Deng, W., Lothe, I.M.B., Couvelard, A., Hjortland, G.O., Sundlöv, A., Svensson, J., et al. (2021). The molecular characteristics of high-grade gastroenteropancreatic neuroendocrine neoplasms. Endocr. Relat. Cancer *29*, 1–14.
16. Sun, T.Y., Zhao, L., Van Hummelen, P., Martin, B., Hornbacker, K., Lee, H., Xia, L.C., Padda, S.K., Ji, H.P., and Kunz, P. (2022). Exploratory genomic analysis of high-grade neuroendocrine neoplasms across diverse primary sites. Endocr. Relat. Cancer *29*, 665–679.
17. Rudin, C.M., Poirier, J.T., Byers, L.A., Dive, C., Dowlati, A., George, J., Heymach, J.V., Johnson, J.E., Lehman, J.M., MacPherson, D., et al. (2019). Molecular subtypes of small cell lung cancer: a synthesis of human and mouse model data. Nat. Rev. Cancer *19*, 289–297.
18. Karpathakis, A., Dibra, H., Pipinikas, C., Feber, A., Morris, T., Francis, J., Oukrif, D., Mandair, D., Pericleous, M., Mohmaduvesh, M., et al. (2016). Prognostic Impact of Novel Molecular Subtypes of Small Intestinal Neuroendocrine Tumor. Clin. Cancer Res. *22*, 250–258.
19. Sadanandam, A., Wullschleger, S., Lyssiotis, C.A., Grötzinger, C., Barbi, S., Bersani, S., Körner, J., Wafy, I., Mafficini, A., Lawlor, R.T., et al. (2015). A Cross-Species Analysis in Pancreatic Neuroendocrine Tumors Reveals Molecular Subtypes with Distinctive Clinical, Metastatic, Developmental, and Metabolic Characteristics. Cancer Discov. *5*, 1296–1313.
20. Wang, Z., Liu, C., Zheng, S., Yao, Y., Wang, S., Wang, X., Yin, E., Zeng, Q., Zhang, C., Zhang, G., et al. (2024). Molecular subtypes of neuroendocrine carcinomas: A cross-tissue classification framework based on five transcriptional regulators. Cancer Cell *42*, 1106–1125.e8.
21. Boilève, A., Faron, M., Fodil-Cherif, S., Bayle, A., Lamartina, L., Planchard, D., Tselikas, L., Kanaan, C., Scoazec, J.Y., Ducreux, M., et al. (2023). Molecular profiling and target actionability for precision medicine in neuroendocrine neoplasms: real-world data. Eur. J. Cancer *186*, 122–132.
22. Raj, N., Shah, R., Stadler, Z., Mukherjee, S., Chou, J., Untch, B., Li, J., Kelly, V., Saltz, L.B., Mandelker, D., et al. (2018). Real-Time Genomic Characterization of Metastatic Pancreatic Neuroendocrine Tumors Has Prognostic Implications and Identifies Potential Germline Actionability. JCO Precis. Oncol. *2018*. https://doi.org/10.1200/PO.17.00267.
23. Vijayvergia, N., Boland, P.M., Handorf, E., Gustafson, K.S., Gong, Y., Cooper, H.S., Sheriff, F., Astsaturov, I., Cohen, S.J., and Engstrom, P.F. (2016). Molecular profiling of neuroendocrine malignancies to identify prognostic and therapeutic markers: a Fox Chase Cancer Center Pilot Study. Br. J. Cancer *115*, 564–570.
24. Williamson, L.M., Steel, M., Grewal, J.K., Thibodeau, M.L., Zhao, E.Y., Loree, J.M., Yang, K.C., Gorski, S.M., Mungall, A.J., Mungall, K.L., et al. (2019). Genomic characterization of a well-differentiated grade 3 pancreatic neuroendocrine tumor. Cold Spring Harb. Mol. Case Stud. *5*, a003814. https://doi.org/10.1101/mcs.a003814.
25. Wong, H.-L., Yang, K.C., Shen, Y., Zhao, E.Y., Loree, J.M., Kennecke, H.F., Kalloger, S.E., Karasinska, J.M., Lim, H.J., Mungall, A.J., et al. (2018). Molecular characterization of metastatic pancreatic neuroendocrine tumors (PNETs) using whole-genome and transcriptome sequencing. Cold Spring Harb. Mol. Case Stud. *4*, a002329. https://doi.org/10.1101/mcs.a002329.
26. Fazio, N., and La Salvia, A. (2023). Precision medicine in gastroenteropancreatic neuroendocrine neoplasms: Where are we in 2023? Best Pract. Res. Clin. Endocrinol. Metab. *37*, 101794.
27. Mock, A., Teleanu, M.-V., Kreutzfeldt, S., Heilig, C.E., Hüllein, J., Möhrmann, L., Jahn, A., Hanf, D., Kerle, I.A., Singh, H.M., et al. (2023). NCT/DKFZ MASTER handbook of interpreting whole-genome, transcriptome, and methylome data for precision oncology. npj Precis. Oncol. *7*, 109.
28. Alexandrov, L.B., Nik-Zainal, S., Wedge, D.C., Aparicio, S.A.J.R., Behjati, S., Biankin, A.V., Bignell, G.R., Bolli, N., Borg, A., Børresen-Dale, A.-L., et al. (2013). Signatures of mutational processes in human cancer. Nature *500*, 415–421.
29. Girard, N., Mazieres, J., Otto, J., Lena, H., Lepage, C., Egenod, T., Smith, D., Madelaine, J., Gérinière, L., El Hajbi, F., et al. (2021). LBA41 Nivolumab (nivo) ± ipilimumab (ipi) in pre-treated patients with advanced, refractory pulmonary or gastroenteropancreatic poorly differentiated neuroendocrine tumors (NECs) (GCO-001 NIPINEC). Ann. Oncol. *32*, S1318.
30. Owen, D.H., Benner, B., Wei, L., Sukrithan, V., Goyal, A., Zhou, Y., Pilcher, C., Suffren, S.-A., Christenson, G., Curtis, N., et al. (2023). A Phase II Clinical Trial of Nivolumab and Temozolomide for Neuroendocrine Neoplasms. Clin. Cancer Res. *29*, 731–741.
31. Patel, S.P., Othus, M., Chae, Y.K., Giles, F.J., Hansel, D.E., Singh, P.P., Fontaine, A., Shah, M.H., Kasi, A., Baghdadi, T.A., et al. (2020). A Phase II Basket Trial of Dual Anti-CTLA-4 and Anti-PD-1 Blockade in Rare Tumors (DART SWOG 1609) in Patients with Nonpancreatic Neuroendocrine Tumors. Clin. Cancer Res. *26*, 2290–2296.
32. Strosberg, J., Mizuno, N., Doi, T., Grande, E., Delord, J.-P., Shapira-Frommer, R., Bergsland, E., Shah, M., Fakih, M., Takahashi, S., et al. (2020). Efficacy and Safety of Pembrolizumab in Previously Treated Advanced Neuroendocrine Tumors: Results From the Phase II KEYNOTE-158 Study. Clin. Cancer Res. *26*, 2124–2130.
33. Yao, J.C., Strosberg, J., Fazio, N., Pavel, M.E., Bergsland, E., Ruszniewski, P., Halperin, D.M., Li, D., Tafuto, S., Raj, N., et al. (2021). Spartalizumab in metastatic, well/poorly differentiated neuroendocrine neoplasms. Endocr. Relat. Cancer *28*, 161–172.

34. Kaufman, H.L., Russell, J., Hamid, O., Bhatia, S., Terheyden, P., D'Angelo, S.P., Shih, K.C., Lebbé, C., Linette, G.P., Milella, M., et al. (2016). Avelumab in patients with chemotherapy-refractory metastatic Merkel cell carcinoma: a multicentre, single-group, open-label, phase 2 trial. Lancet Oncol. *17*, 1374–1385.

35. de Mestier du Bourg, L., Cohen, D., Masliah-Planchon, J., Sivakumar, S., De rycke, O., Dhome, O.H., Fleischmann, Z., Sokol, E.S., Decker, B., Couvelard, A., et al. (2023). 1182O Temozolomide treatment induces an MMR-dependent hypermutator phenotype in well differentiated pancreatic neuroendocrine tumors. Ann. Oncol. *34*, S701.

36. Klempner, S.J., Hendifar, A., Waters, K.M., Nissen, N., Vail, E., Tuli, R., and Mita, A. (2020). Exploiting Temozolomide-Induced Hypermutation With Pembrolizumab in a Refractory High-Grade Neuroendocrine Neoplasm: A Proof-of-Concept Case. JCO Precis. Oncol. *4*, 614–619.

37. Sun, F., Grenert, J.P., Tan, L., Van Ziffle, J., Joseph, N.M., Mulvey, C.K., and Bergsland, E. (2022). Checkpoint Inhibitor Immunotherapy to Treat Temozolomide-Associated Hypermutation in Advanced Atypical Carcinoid Tumor of the Lung. JCO Precis. Oncol. *6*, e2200009.

38. Vitiello, P.P., Rousseau, B., Chilà, R., Battuello, P., Amodio, V., Battaglieri, V., Grasso, G., Scardellato, S., Anselmo, A., Clemente, F., et al. (2025). Cisplatin and temozolomide combinatorial treatment triggers hypermutability and immune surveillance in experimental cancer models. Cancer Cell *43*, 1296–1312.e7.

39. Klempner, S.J., Gershenhorn, B., Tran, P., Lee, T.K., Erlander, M.G., Gowen, K., Schrock, A.B., Morosini, D., Ross, J.S., Miller, V.A., et al. (2016). BRAFV600E Mutations in High-Grade Colorectal Neuroendocrine Tumors May Predict Responsiveness to BRAF-MEK Combination Therapy. Cancer Discov. *6*, 594–600.

40. Park, C., Ha, S.Y., Kim, S.T., Kim, H.C., Heo, J.S., Park, Y.S., Lauwers, G., Lee, J., and Kim, K.-M. (2016). Identification of the BRAF V600E mutation in gastroenteropancreatic neuroendocrine tumors. Oncotarget *7*, 4024–4035.

41. Pishvaian, M.J., Blais, E.M., Brody, J.R., Rahib, L., Lyons, E., De Arbeloa, P., Hendifar, A., Mikhail, S., Chung, V., Sohal, D.P.S., et al. (2019). Outcomes in Patients With Pancreatic Adenocarcinoma With Genetic Mutations in DNA Damage Response Pathways: Results From the Know Your Tumor Program. JCO Precis. Oncol. *3*, 1–10.

42. Tsang, E.S., Csizmok, V., Williamson, L.M., Pleasance, E., Topham, J.T., Karasinska, J.M., Titmuss, E., Schrader, I., Yip, S., Tessier-Cloutier, B., et al. (2023). Homologous recombination deficiency signatures in gastrointestinal and thoracic cancers correlate with platinum therapy duration. npj Precis. Oncol. *7*, 31.

43. van Riet, J., van de Werken, H.J.G., Cuppen, E., Eskens, F.A.L.M., Tesselaar, M., van Veenendaal, L.M., Klümpen, H.-J., Dercksen, M.W., Valk, G.D., Lolkema, M.P., et al. (2021). The genomic landscape of 85 advanced neuroendocrine neoplasms reveals subtype-heterogeneity and potential therapeutic targets. Nat. Commun. *12*, 4612.

44. Yachida, S., Totoki, Y., Noë, M., Nakatani, Y., Horie, M., Kawasaki, K., Nakamura, H., Saito-Adachi, M., Suzuki, M., Takai, E., et al. (2022). Comprehensive Genomic Profiling of Neuroendocrine Carcinomas of the Gastrointestinal System. Cancer Discov. *12*, 692–711.

45. Miyazawa, S., Ono, H., Yamashita, H., Asano, D., Ishikawa, Y., Watanabe, S., Ueda, H., Aoyama, S., Ishibashi, N., Akahoshi, K., et al. (2025). Evaluation of therapeutic agent selection based on comprehensive genomic profiling in gastroenteropancreatic neuroendocrine neoplasms. PLoS One *20*, e0325727.

46. Liu, M., Li, N., Tang, H., Chen, L., Liu, X., Wang, Y., Lin, Y., Luo, Y., Wei, S., Wen, W., et al. (2023). The Mutational, Prognostic, and Therapeutic Landscape of Neuroendocrine Neoplasms. Oncologist *28*, e723–e736.

47. Liu, J., Zhong, M., Yang, K., Wang, J., Ma, H., Wang, W., Sun, L., Liu, L., Xu, J., Cui, X., et al. (2025). Proteomics analysis reveals FEN1 as a promising therapeutic target against small cell neuroendocrine carcinoma of the cervix. Sci. Rep. *15*, 27827.

48. Cavalcanti, E., Scalavino, V., Vincenti, L., Piccinno, E., De Marinis, L., Armentano, R., and Serino, G. (2025). Identification of miRNA/FGFR2 Axis in Well-Differentiated Gastroenteropancreatic Neuroendocrine Tumors. Int. J. Mol. Sci. *26*, 7232. https://doi.org/10.3390/ijms26157232.

49. Massironi, S., Facciotti, F., Cavalcoli, F., Amoroso, C., Rausa, E., Centonze, G., Cribiù, F.M., Invernizzi, P., and Milione, M. (2022). Intratumor Microbiome in Neuroendocrine Neoplasms: A New Partner of Tumor Microenvironment? A Pilot Study. Cells *11*, 692. https://doi.org/10.3390/cells11040692.

50. Galasso, L., Vitale, F., Giansanti, G., Esposto, G., Borriello, R., Mignini, I., Nicoletti, A., Zileri Dal Verme, L., Gasbarrini, A., Ainora, M.E., and Zocco, M.A. (2025). Decoding Pancreatic Neuroendocrine Tumors: Molecular Profiles, Biomarkers, and Pathways to Personalized Therapy. Int. J. Mol. Sci. *26*, 7814. https://doi.org/10.3390/ijms26167814.

51. Dickson, D., Johnson, J., Bergan, R., Owens, R., Subbiah, V., and Kurzrock, R. (2020). The Master Observational Trial: A New Class of Master Protocol to Advance Precision Medicine. Cell *180*, 9–14.

52. Li, H. (2013). Aligning sequence reads, clone sequences and assembly contigs with BWA-MEM. Preprint at arXiv. https://doi.org/10.48550/ARXIV.1303.3997.

53. Tischler, G., and Leonard, S. (2014). biobambam: tools for read pair collation based algorithms on BAM files. Source Code. Biol. Med. *9*, 13.

54. Tarasov, A., Vilella, A.J., Cuppen, E., Nijman, I.J., and Prins, P. (2015). Sambamba: fast processing of NGS alignment formats. Bioinformatics *31*, 2032–2034.

55. Danecek, P., Bonfield, J.K., Liddle, J., Marshall, J., Ohan, V., Pollard, M.O., Whitwham, A., Keane, T., McCarthy, S.A., Davies, R.M., and Li, H. (2021). Twelve years of SAMtools and BCFtools. GigaScience *10*, giab008. https://doi.org/10.1093/gigascience/giab008.

56. Wang, K., Li, M., and Hakonarson, H. (2010). ANNOVAR: functional annotation of genetic variants from high-throughput sequencing data. Nucleic Acids Res. *38*, e164.

57. Rimmer, A., Phan, H., Mathieson, I., Iqbal, Z., Twigg, S.R.F., WGS500 Consortium; Wilkie, A.O.M., McVean, G., and Lunter, G. (2014). Integrating mapping-assembly- and haplotype-based approaches for calling variants in clinical sequencing applications. Nat. Genet. *46*, 912–918.

58. Toprak, U. (2019). Integrative Analysis of Omics Datasets (Heidelberg University Library). https://doi.org/10.11588/HEIDOK.00027429.

59. Kleinheinz, K., Bludau, I., Hübschmann, D., Heinold, M., Kensche, P., Gu, Z., López, C., Hummel, M., Klapper, W., Möller, P., et al. (2017). ACEseq – allele specific copy number estimation from whole genome sequencing. Preprint at bioRxiv. https://doi.org/10.1101/210807.

60. Talevich, E., Shain, A.H., Botton, T., and Bastian, B.C. (2016). CNVkit: Genome-Wide Copy Number Detection and Visualization from Targeted DNA Sequencing. PLoS Comput. Biol. *12*, e1004873.

61. Mermel, C.H., Schumacher, S.E., Hill, B., Meyerson, M.L., Beroukhim, R., and Getz, G. (2011). GISTIC2.0 facilitates sensitive and confident localization of the targets of focal somatic copy-number alteration in human cancers. Genome Biol. *12*, R41.

62. Gu, Z., Gu, L., Eils, R., Schlesner, M., and Brors, B. (2014). circlize Implements and enhances circular visualization in R. Bioinformatics *30*, 2811–2812.

63. Hübschmann, D., Jopp-Saile, L., Andresen, C., Krämer, S., Gu, Z., Heilig, C.E., Kreutzfeldt, S., Teleanu, V., Fröhling, S., Eils, R., and Schlesner, M. (2021). Analysis of mutational signatures with yet another package for signature analysis. Genes Chromosomes Cancer *60*, 314–331.

64. Jia, P., Yang, X., Guo, L., Liu, B., Lin, J., Liang, H., Sun, J., Zhang, C., and Ye, K. (2020). MSIsensor-pro: Fast, Accurate, and Matched-normal-sample-free Detection of Microsatellite Instability. Genom. Proteom. Bioinform. *18*, 65–71.

65. Dobin, A., Davis, C.A., Schlesinger, F., Drenkow, J., Zaleski, C., Jha, S., Batut, P., Chaisson, M., and Gingeras, T.R. (2013). STAR: ultrafast universal RNA-seq aligner. Bioinformatics *29*, 15–21.

66. Uhrig, S., Ellermann, J., Walther, T., Burkhardt, P., Fröhlich, M., Hutter, B., Toprak, U.H., Neumann, O., Stenzinger, A., Scholl, C., et al. (2021). Accurate and efficient detection of gene fusions from RNA sequencing data. Genome Res. *31*, 448–460.

67. Gu, Z., Schlesner, M., and Hübschmann, D. (2021). cola: an R/Bioconductor package for consensus partitioning through a general framework. Nucleic Acids Res. *49*, e15.

68. [No tite] https://cran.r-project.org/doc/manuals/r-release/fullrefman.pdf.

69. Wickham, H., Averick, M., Bryan, J., Chang, W., McGowan, L., François, R., Grolemund, G., Hayes, A., Henry, L., Hester, J., et al. (2019). Welcome to the tidyverse. J. Open Source Softw. *4*, 1686.

70. Gu, Z., Eils, R., and Schlesner, M. (2016). Complex heatmaps reveal patterns and correlations in multidimensional genomic data. Bioinformatics *32*, 2847–2849.

71. Ramos, M., Schiffer, L., Re, A., Azhar, R., Basunia, A., Rodriguez, C., Chan, T., Chapman, P., Davis, S.R., Gomez-Cabrero, D., et al. (2017). Software for the Integration of Multiomics Experiments in Bioconductor. Cancer Res. *77*, e39–e42.

72. Lawrence, M.S., Stojanov, P., Polak, P., Kryukov, G.V., Cibulskis, K., Sivachenko, A., Carter, S.L., Stewart, C., Mermel, C.H., Roberts, S.A., et al. (2013). Mutational heterogeneity in cancer and the search for new cancer-associated genes. Nature *499*, 214–218.

73. Leichsenring, J., Horak, P., Kreutzfeldt, S., Heining, C., Christopoulos, P., Volckmar, A.-L., Neumann, O., Kirchner, M., Ploeger, C., Budczies, J., et al. (2019). Variant classification in precision oncology. Int. J. Cancer *145*, 2996–3010.

74. Lier, A., Penzel, R., Heining, C., Horak, P., Fröhlich, M., Uhrig, S., Budczies, J., Kirchner, M., Volckmar, A.-L., Hutter, B., et al. (2018). Validating Comprehensive Next-Generation Sequencing Results for Precision Oncology: The NCT/DKTK Molecularly Aided Stratification for Tumor Eradication Research Experience. JCO Precis. Oncol. *2*, 1–13.

75. Sondka, Z., Bamford, S., Cole, C.G., Ward, S.A., Dunham, I., and Forbes, S.A. (2018). The COSMIC Cancer Gene Census: describing genetic dysfunction across all human cancers. Nat. Rev. Cancer *18*, 696–705.

76. Abkevich, V., Timms, K.M., Hennessy, B.T., Potter, J., Carey, M.S., Meyer, L.A., Smith-McCune, K., Broaddus, R., Lu, K.H., Chen, J., et al. (2012). Patterns of genomic loss of heterozygosity predict homologous recombination repair defects in epithelial ovarian cancer. Br. J. Cancer *107*, 1776–1782.

77. Popova, T., Manié, E., Rieunier, G., Caux-Moncoutier, V., Tirapo, C., Dubois, T., Delattre, O., Sigal-Zafrani, B., Bollet, M., Longy, M., et al. (2012). Ploidy and large-scale genomic instability consistently identify basal-like breast carcinomas with BRCA1/2 inactivation. Cancer Res. *72*, 5454–5462.

78. Birkbak, N.J., Wang, Z.C., Kim, J.-Y., Eklund, A.C., Li, Q., Tian, R., Bowman-Colin, C., Li, Y., Greene-Colozzi, A., Iglehart, J.D., et al. (2012). Telomeric allelic imbalance indicates defective DNA repair and sensitivity to DNA-damaging agents. Cancer Discov. *2*, 366–375.

79. 1000 Genomes Project Consortium; Auton, A., Brooks, L.D., Durbin, R.M., Garrison, E.P., Kang, H.M., Korbel, J.O., Marchini, J.L., McCarthy, S., McVean, G.A., and Abecasis, G.R. (2015). A global reference for human genetic variation. Nature *526*, 68–74.

80. Kaplan Meier and Log Rank https://www.statskingdom.com/kaplan-meier.html.

STAR★METHODS

KEY RESOURCES TABLE

REAGENT or RESOURCE	SOURCE	IDENTIFIER
Deposited data		
Raw DNA/RNA sequencing data	This paper	German Human Genome-Phenome Archive: GHGAS82588167690104
Software and algorithms		
BWA mem version 0.7.15	Li et al.[52]	https://github.com/lh3/bwa/tree/v0.7.15
Bamsort, biobambam package version 0.0.148	Tischler et al.[53]	https://github.com/gt1/biobambam/tree/0.0.148-release-20140618101902
Markdup, sambamba package version 0.6.5	Tarasov et al.[54]	https://github.com/biod/sambamba/releases/tag/v0.6.5
Mpileup, BCFtools, SAMtools version 0.1.19	Danecek et al.[55]	https://github.com/samtools/samtools/tree/0.1.19
ANNOVAR version November 2014 and version February 2016	Wang et al.[56]	https://annovar.openbioinformatics.org/en/latest/user-guide/download/
Platypus version 0.8.1	Rimmer et al.[57]	https://github.com/andyrimmer/Platypus/tree/master/release/AllReleases
SOPHIA version 2.2.0	Toprak 2019[58]	https://github.com/DKFZ-ODCF/SophiaWorkflow/tree/2.2.0?tab=readme-ov-file
ACEseq version 5.1.0	Kleinheinz et al.[59]	https://github.com/DKFZ-ODCF/ACEseqWorkflow
CNVkit version 0.9.3	Talevich et al.[60]	https://github.com/etal/cnvkit/tree/v0.9.3
GISTIC version 2.0.23	Mermel et al.[61]	https://github.com/broadinstitute/gistic2/tree/v2.0.23
Circlize version 0.4.16	Gu et al.[62]	https://github.com/jokergoo/circlize
YAPSA version 1.14.0	Hübschmann et al.[63]	https://bioconductor.org/packages/release/bioc/html/YAPSA.html
MSIsensor-pro version 1.2.0	Jia et al.[64]	https://github.com/xjtu-omics/msisensor-pro/tree/v1.2.0
STAR version 2.5.1b	Dobin et al.[65]	https://github.com/alexdobin/STAR/releases/tag/2.5.1b
Arriba version 0.8	Uhrig et al.[66]	https://github.com/suhrig/arriba/tree/v0.8
Cola version 1.9.4	Gu et al.[67]	https://www.bioconductor.org/packages/release/bioc/html/cola.html
R version 4.0.0	R Core Team[68]	https://www.r-project.org/
Tidyverse version 1.3.0	Wickham et al.[69]	https://tidyverse.tidyverse.org/index.html
ComplexHeatmap version 2.21.2	Gu et al.[70]	https://bioconductor.org/packages/release/bioc/html/ComplexHeatmap.html
MultiAssayExperiment version 1.14.0	Ramos et al.[71]	https://www.bioconductor.org/packages/release/bioc/html/MultiAssayExperiment.html
GenomicRanges version 1.40.0	Lawrence et al.[72]	https://bioconductor.org/packages/release/bioc/html/GenomicRanges.html

EXPERIMENTAL MODEL AND STUDY PARTICIPANT DETAILS

Patients

Patients with advanced NENs provided written informed consent for multi-layered molecular profiling of tumor tissue and, in the case of DNA sequencing, a matched blood sample, as well as for the longitudinal collection of clinical information as part of the DKFZ/NCT/

DKTK MASTER program. The study was approved by the Ethics Committee of Heidelberg University (protocol no. S-206/2011) and conducted in accordance with the Declaration of Helsinki. Biological curation and clinical annotation of molecular profiles were performed as previously described,[5,27] and a multi-institutional MTB involving treating physicians provided recommendations for clinical management. Diagnoses and basket assignments were curated based on histopathologic reports and clinical considerations. Prior palliative systemic treatment was documented, whereas neoadjuvant and adjuvant therapies were excluded if administered with curative intent and followed by a progression-free interval of more than six months. Clinical records were collected before and three, six, 12, 18, and 24 months after MTB discussion. Outcome assessments were performed retrospectively by specialists and fellows in medical oncology or human genetics using available clinical documentation. Treatment failure was assessed when a drug had been administered for at least two cycles or, in the case of continuous treatment, for at least one month at a dose of at least 50%. Treatment response was evaluated based on clinical and radiologic reports. Responses were not assessed in cases with missing documentation or confounding therapeutic interventions, e.g., surgery or radiotherapy. Progression-free survival was determined for both prior systemic therapies and treatments implemented according to MTB recommendations. Biomarkers were defined as any tumor- or patient-associated molecular alterations detected by WGS/WES and/or RNA-seq that informed clinical decision-making by the MTB. A description of the cohort is provided in Figure 1. Information on socioeconomic status, race, or ethnicity was not collected. Analyses of sex/gender-based differences were performed with respect to enrollment and age, but not individual NEN subgroups, as most NEN subgroups were too small and heterogeneous to yield meaningful intra-group comparisons.

METHOD DETAILS

Sample processing

Frozen tissue sections were assessed by board-certified pathologists to determine tumor cell content, including the presence of necrosis. Suitable samples were processed further at the NCT Heidelberg Sample Processing Laboratory. DNA and RNA from tumor specimens and DNA from matched blood samples were isolated using the AllPrep DNA/RNA/miRNA Universal Kit and the QIAamp DNA Mini Kit (Qiagen). For formalin-fixed paraffin-embedded (FFPE) samples, nucleic acids were extracted using the Allprep DNA/RNA FFPE kit (Qiagen). Nucleic acid quantification and quality control were performed using a Qubit Fluorometer (Life Technologies) and a 4200 or 2200 TapeStation system (Agilent). Samples were assigned to WGS/WES and RNA-seq based on quality and method availability at the time of analysis. All kits were used according to the manufacturers' instructions.

DNA sequencing

Libraries for WGS were prepared using the Illumina TruSeq Nano DNA Library Prep Kit and sequenced on an Illumina HiSeq X Ten or NovaSeq 6000 instrument at the DKFZ Next Generation Sequencing Core Facility. Libraries for WES were prepared using the Agilent SureSelect All Exon Kit v5, v5 + UTRs, or v6.2 and sequenced on an Illumina HiSeq 2500 or HiSeq 4000 instrument. Reads were mapped to the 1000 Genomes Project phase 2 assembly of the human reference genome (NCBI build 37.1) using BWA mem (version 0.7.15)[52] with default parameters and filtering by alignment score disabled. BAM files were sorted with bamsort (biobambam package version 0.0.148),[53] and duplicates were marked with markdup (Sambamba package version 0.6.5).[54] All kits were used according to the manufacturers' instructions.

Somatic SNV and indel calling

Somatic SNVs were detected with an in-house pipeline based on SAMtools (version 0.1.19) mpileup and bcftools[56] and using heuristic filtering as previously described.[5,73,74] Briefly, initial SNV calls were detected in the tumor BAM file by mpileup, which considered only reads with a minimum mapping quality of 30 (−q30), and bcftools, which reported all positions containing at least one high-quality non-reference base (−vcgN −p2.0), followed by inspection of these positions in the control sample using mpileup. SNVs were annotated with ANNOVAR (version November 2014) using GENCODE (release 19). Downstream filtering discarded variants with low support of the alternative allele, occurring in tandem repeats or other read-attracting regions, with PCR or sequencing strand bias, or with significant bias in the PV4 field of the mpileup output. Somatic SNVs annotated as missense, stopgain, stoploss, or splicing were defined as non-silent. Short indels were detected with Platypus (version 0.8.1.1),[57] and only those that had the filter tag PASS or passed custom filters allowing for low variant frequency were retained. Annotation of indels was performed using ANNOVAR (version February 2016), and calls falling into a coding sequence or splice site were extracted.

Germline SNV and indel calling

Germline SNVs and indels were analyzed as previously described.[5] Briefly, selected variants were required to have a variant allele frequency of at least 30% in the control sample, be absent from common dbSNP annotations, and have a frequency below 0.1% in the 1000 Genomes reference. SNVs with three or more homozygous or 40 or more heterozygous individuals in ExAC were excluded. Additionally, we filtered out variants present in more than 50 individuals from a local control dataset of 280 samples. For indels, the exclusion threshold was 10 in the local controls and 50 in ExAC when there was a unique exact match. If multiple entries or a different indel were present at the same position, the indel was annotated but not removed. Recurrent WGS artifacts were manually removed.

Somatic structural variant calling

Structural variants (SVs) were detected using SOPHIA (version 2.2.0),[58] which uses the "supplementary alignment" feature of BWA mem to discover SVs, along with custom thresholds and a background panel of normals to filter out common variants and recurrent artifacts.

Somatic CNA calling

DNA copy number profiles of samples subjected to WGS or WES were determined using ACEseq (version: 5.1.0)[59] and CNVkit (version: 0.9.3),[59,60] respectively. An amplification was called when the copy number of a given segment exceeded two times the sample ploidy plus one. Significantly amplified or deleted genomic regions were identified using GISTIC (version 2.0.23)[61] with additional settings (−ta 0.4 −td 0.4 −cap 2 −maxseg 3500). The boundaries of each significant amplification or deletion ("Region Limits") were then intersected with the location of genes from the Cancer Gene Census.[75] Results were visualized using the circlize R package (version 0.4.16).[62]

TMB quantification

The number of mut/Mb was calculated by dividing the sum of non-silent SNVs and coding indels by the length of the genome's coding sequence. For WES samples, the denominator was adjusted to the respective target coverage.

Mutational signature analysis

The presence of mutational signatures from the COSMIC database (version 2)[28] was assessed using the YAPSA R package (version 1.14.0).[63] The analysis included all high-confidence somatic SNVs, limited to those within target regions for WES samples. Samples containing 50 or fewer SNVs were excluded. For each sample, a mutation catalog was generated and normalized to the length of the targeted genome, followed by signature decomposition. Signatures were considered present if they exceeded signature-specific thresholds with a cost factor of 6 and the lower limit of their confidence interval was greater than zero.

HRD scoring

A method to estimate HRD, including large-scale state transition (LST) and telomeric allelic imbalance (TAI) scores, was based on the output of the CNVkit and ACEseq pipelines and computed using methods established for the detection of loss-of-heterozygosity (LOH)[76] and the numbers of LSTs[77] and TAIs.[78] Briefly, copy number profiles were smoothed to reduce oversegmentation caused by technical noise. Adjacent segments with identical rounded total and allele-specific copy numbers that differed by no more than 0.3 were merged. In addition, segments <3 Mbp were merged with the most similar neighboring segment. LSTs were defined as switches between copy number states of segments >10 Mbp that did not correspond to entire chromosome arms. For LOH estimation, segments >15 Mbp that were smaller than a full chromosome and exhibited LOH were counted.

MSI detection

MSI was investigated using MSIsensor-pro (version 1.2.0).[64] The 1000 Genomes reference was used to compile a list of homopolymers and microsatellites for a total of 33,386,244 loci.[79] The minimum required coverage was set to 15 for exomes and 20 for genomes in both tumor and control samples. Samples with scores greater than 3.5 were considered microsatellite unstable.

RNA-seq and gene fusion detection

Libraries were prepared using the Illumina TruSeq RNA Library Preparation Kit or the Illumina TruSeq mRNA Stranded Library Preparation Kit according to the manufacturers' instructions and sequenced on an Illumina HiSeq 2500, HiSeq 4000, HiSeq X Ten, or NovaSeq 6000 instrument. Reads were aligned to the same reference genome as DNA sequencing data with STAR 2.5.2b.[65] Gene fusions were obtained using Arriba (version 0.8).[66]

RNA-based clustering

Unsupervised clustering of samples was performed on log2 of TPM+1 values using the cola R package (version 1.9.4),[67] incorporating all genes with at least ten counts in at least 10% of samples. Consensus partitioning yielding five clusters was selected based on its stability and uniform sample distribution, utilizing standard deviation as the top-value method and skmeans as the partitioning method.

QUANTIFICATION AND STATISTICAL ANALYSIS

The differential prevalence of mutations between primary tumor sites and histopathologic subgroups was assessed using Fisher's exact test (significance threshold of $p < 0.05$). Unless otherwise specified, comparisons were made between the indicated group and all remaining samples. Specific p-values for enrichment of individual gene alterations across histopathologic subtypes and primary sites are reported in the Results and in Figures 2A and S1B. Differences in TMB between NEN subgroups were assessed using the Wilcoxon rank-sum test (significance threshold of $p < 0.05$), with results and p-values reported in the Results section and in Figure S1A. For all statistical comparisons, n denotes the number of patients, and subgroup-specific sample sizes are detailed in

the Results section, Figure 1B, and Table S1. Key subgroup sizes include NEC (n = 75), MiNEN (n = 21), G3 NET (n = 22), and G1/2 NET (n = 48), with 160 patients (NEC, n = 75; MiNEN, n = 19; G3 NET, n = 22; G1/2 NET, n = 44) contributing high-quality sequencing data (WGS, n = 84; WES, n = 76; RNA-seq, n = 105). These were used for Fisher's and Wilcoxon tests. Kaplan-Meier survival analyses, including log rank tests, were conducted using the online tool Statistics Kingdom[80] (significance threshold of $p < 0.05$). Overall survival was compared between patients who received MTB-recommended therapies and those who received other, non-MTB-recommended therapies, both in the full cohort and stratified by histopathologic subtype. Patient numbers and results are included in the Results and/or in Figures S3A–S3C. Descriptive statistics are reported as median and range throughout. Continuous variables such as age at enrollment, number of prior palliative therapies, TMB, and number of biomarkers per recommendation are summarized accordingly. These values are reported in the Results section and corresponding figures. Response to MTB-recommended therapies was evaluated based on clinical and radiologic reports (best response per therapy and duration of tumor control). Response data, including individual patient-level outcomes and progression-free survival, are presented in Figures 5, 6, and 7 and summarized in Table S3. Treatment- and patient-level clinical benefit rates are reported in the Results. No formal power calculation was performed, as the study included all patients with a diagnosis of epithelial NEN enrolled in the MASTER program. Given the rarity and heterogeneity of NENs, several subtype- and site-specific subgroups are small, and all molecular and clinical findings should be regarded as exploratory and hypothesis-generating, as noted in the Limitations section. Analyses were performed in R (version 4.0.0) using Bioconductor or CRAN packages, including tidyverse (version 1.3.0),[69] ComplexHeatmap (version 2.21.2),[70] MultiAssayExperiment (version 1.14.0),[71] GenomicRanges (version 1.40.0).[72]

ADDITIONAL RESOURCES

Further information on the MASTER program: https://www.nct-heidelberg.de/master.

Clinical trial registration information on the MASTER observational trial (NCT05852522): https://clinicaltrials.gov/study/NCT05852522?term=NCT05852522&rank=1.